Thesis:

Effects of Early Life Stress on Fear-induced Glutamate Release and Activity of Parvalbumin Interneurons in the Medial Prefrontal Cortex of Pre-Adolescent Rats.

Jiamin Song

Department of Psychiatry, McGill University, Montreal

November 2021

A thesis submitted to McGill University in partial fulfillment of the requirements of the degree of Master of Science

Table of Contents

I. Abstract (English)

Exposure to early life stress (ELS) can exert long-lasting impacts on emotional regulation and cognitive abilities. The medial prefrontal cortex (mPFC) is crucial in fear regulation and is highly susceptible to early adversities. Using a limited bedding (LB) paradigm between postnatal days (PND)1-10 to induce chronic ELS, we examined the functional consequences of ELS on the prelimbic (PL or dmPFC) and infralimbic (IL or vmPFC) mPFC during fear conditioning in the pre-adolescent offspring. We measured fear-induced glutamatergic transmission in the mPFC using *in vivo* microdialysis in behaving pre-adolescent male and female (PND28-32) and adult male rats. Compared to normal bedding (NB) controls, fear-induced glutamate release in the PL, but not IL mPFC tended to be diminished in LB male, but not female pre-adolescent offspring, whereas the prelimbic glutamate response to fear conditioning was enhanced in LB-exposed adult males. The glutamatergic projections that target the mPFC are regulated by the activity of local inhibitory interneurons, including parvalbumin (PV) expressing cells. To estimate the effects of LB on the fear-related activity of PV interneurons and their maturational state in the mPFC of pre-adolescents, we used triple fluorescence immunostaining to quantify the density of PV cells co-expressing cFos and perineuronal nets (PNNs). Formation of PNNs around PV interneurons is associated with a mature state of PV interneurons. LB exposure reduced the density of cells co-expressing PV and PNN in the PL and IL mPFC of male, but not female offspring. These results suggest that ELS modifies the programming of glutamatergic neurotransmission in the mPFC during fear conditioning and the maturation of prefrontal PV interneurons in a sex- and region-specific pattern, possibly reflecting the differential maturational state of excitatory mPFC inputs and local inhibitory circuits in the ELS-exposed pre-adolescent rats. This work was supported by CIHR PJT#162376 to CDW.

II. Abstract (French)

L'exposition au stress précoce (ELS) peut avoir des effets durables sur la régulation émotionnelle et les capacités cognitives des individus. Le cortex préfrontal médian (mPFC) joue un rôle important dans la régulation de la peur et est très sensible à l'adversité périnatale. Nous avons déterminé les conséquences fonctionnelles du stress précoce sur la neurotransmission glutamatergique dans le mPFC prélimbique (PL) et infralimbique (IL) pendant le conditionnement de la peur chez la progéniture pré-adolescente (PND28-32) et adulte. Nous avons simulé l'adversité périnatale en utilisant un paradigme connu qui consiste à limiter l'accès à de la literie pendant les dix premiers jours de vie postnatale (LB). Nous avons mesuré la transmission glutamatergique induite par la peur dans le mPFC en utilisant la microdialyse *in vivo* et quantifié le comportement de peur des rats pré-adolescents. Par rapport aux témoins contrôles (NB), la libération de glutamate induite par la peur dans le mPFC PL, mais pas le mPFC IL, avait tendance à être diminuée chez les préadolescents mâles, mais pas chez les femelles LB. Chez les males adultes, la relation inverse est observée dans le PL mPFC avec une augmentation de la réponse glutamatergique chez les animaux en LB compare aux contrôles. Le comportement de « freezing » suite au conditionnement a la peur était également augmente chez les rats males LB. Les projections glutamatergiques qui ciblent le mPFC sont régulées par l'activité des interneurones inhibiteurs locaux, incluant les cellules exprimant la parvalbumine (PV). Afin d'estimer les effets du stress précoce sur l'activation des interneurones PV et leur état de maturation dans le mPFC des pré-adolescents, nous avons utilisé un triple marquage fluorescent immunohistochimique pour quantifier la densité de cellules PV exprimant cFos et les réseaux périneuronaux (PNN), respectivement. La formation de PNN autour des interneurones PV est associée à la maturation de ces cellules. L'exposition au LB a réduit la densité des cellules co-exprimant PV et PNN dans PL

et IL mPFC de la progéniture mâle, mais pas femelle. Ces résultats suggèrent que le stress précoce modifie la programmation de la neurotransmission glutamatergique dans le mPFC pendant le conditionnement de la peur et la maturation des interneurones PV préfrontaux selon des modèles dépendant du sexe et de la région. Ces effets pourraient peut-être refléter le statut de maturation différentiel des afférences excitatrices ciblant le mPFC ou celui des circuits inhibiteurs locaux. Ces travaux ont été financés par les IRSC (PJT162376) à CDW.

III. Acknowledgements

Foremost, I would like to express my sincere gratitude to Dr. Claire-Dominique Walker for her exceptional supervision throughout this research project and the thesis-writing process. She has guided the experimental design and demonstrated the methodology to conduct the experiments as well as to present the results. I am deeply inspired by her enthusiasm for research and extremely grateful for her patience, encouragement, and empathy during the past two years. It was a great privilege and honor to study under her supervision.

I would like to acknowledge Luc Moquin, our collaborating research technician, who provided invaluable assistance with microdialysis probes, equipment set-up, and HPLC assays. I would like to thank our laboratory technicians Hong Long and Silvanna Verlezza, who provided continued support with surgeries, sample and tissue collections, and immunostaining. Last but not least, I would like to acknowledge Alyssa Guerra for her quantification and analysis of immunostaining data in the PL mPFC.

IV. Contribution of authors

Jiamin Song and Dr. Claire-Dominique Walker designed the experiments. Jiamin Song performed the experiments with the help of: Luc Moquin (microdialysis probes and set up and HPLC analyses), Hong Long, Silvanna Verlezza (microdialysis sampling and immunohistochemistry standardization), and Dr. Claire-Dominique Walker (microdialysis sampling). Jiamin Song and Alyssa Guerra analyzed the immunohistochemistry data. Jiamin Song performed all statistical analyses and wrote the thesis. Dr. Claire-Dominique Walker oversaw data collection and analyses and edited the thesis.

A. Introduction

Exposure to early life stress (ELS) can induce long-term vulnerabilities to psychiatric disorders associated with emotional dysregulation and cognitive deficits, including anxiety, posttraumatic stress disorder (PTSD), and depression (VanTieghem & Tottenham, 2018). The structural and functional consequences of early adversity on the emotion circuitry programming have been documented in both humans and rodents (Pechtel & Pizzagalli, 2011; Bolton *et al.*, 2017; Herzberg & Gunnar, 2020). The corticolimbic system, including the projections from the basolateral amygdala (BLA) and ventral hippocampus (vHIP) to both the prelimbic (PL or dmPFC) and infralimbic (IL or vmPFC) regions of the medial prefrontal cortex (mPFC), plays a key role in fear regulation (Giustino & Maren, 2015). Maturation of this circuitry occurs during the early postnatal and juvenile period, and as a consequence, it is extremely sensitive to environmental stressors throughout early development (Zimmermann *et al.*, 2019). Although the mPFC receives long-range glutamatergic projections that originate from various brain regions, including but not limited to other cortical areas, thalamus, vHIP, and BLA (Anastasiades & Carter, 2021), the fear-induced glutamate response in the mPFC is thought to be primarily mediated by the activation of BLA and vHIP inputs (Tovote *et al.*, 2015). During fear learning and expression, the afferents from the BLA and the vHIP drive both excitatory inputs onto pyramidal neurons and feedforward inhibition via local inhibitory microcircuits in the mPFC (Lucas & Clem, 2018). The activity of parvalbumin (PV) interneurons in the mPFC, in addition to other local GABAergic interneurons, gates the excitatory limbic-prefrontal projections underlying fear learning (Yang *et al.*, 2021). Maturation of PV interneurons coincides with the formation of perineuronal nets (PNNs) in the postnatal period (Guadagno *et al.*, 2021), in part contributing to the unique vulnerability of these cells to the profound effects of ELS. Several models of early life stress in rodents, including the

limited bedding (LB) paradigm used in the present studies (Walker *et al.*, 2017), have been shown to change the morphological and functional characteristics of BLA neurons in pre-adolescent male rats and enhance fear expression later in adulthood (Guadagno *et al.*, 2018b; Guadagno *et al.*, 2020). Thus, alterations in the activity of the BLA after ELS exposure might exert a "bottom-up" effect on the development of the mPFC and the functional consequences of this region in terms of fear learning and expression via glutamatergic projections. However, it is currently unknown to which extent ELS modifies the glutamate response to fear conditioning in the mPFC and whether PV interneurons are actively recruited to modulate pyramidal cell activity under these conditions in pre-adolescent rats. The aims of my project are to examine the effects of ELS on fear-induced glutamatergic transmission in the IL and PL regions of the mPFC and to determine whether ELS modifies the maturation and fear-related activity of PV interneurons in these regions.

Sex-dependent effects of early life stress

The effects of ELS on the corticolimbic circuit have been found to be sex-dependent, with a more pronounced impact on male offspring compared to female offspring in rodents (Walker CD et al. 2017; Guadagno A et al., 2021). It has been well documented that anxiety and fear behavior are enhanced by LB exposure in adult male, but not female rats and mice (Arp *et al.*, 2016; Prusator & Greenwood-Van Meerveld, 2016; Guadagno *et al.*, 2018b; Guadagno *et al.*, 2020). Exposure to unpredictable varied stressors during the period spanning the late postnatal and early juvenile period (PND14-25) has been found to increase connectivity between the amygdala, vHIP and mPFC in adult male, but not female offspring (Johnson *et al.*, 2018; White *et al.*, 2020). Following an intermittent maternal separation during the first two weeks (3h/day, PND3-16), cortical oscillations in the PFC diminish in male but not female juvenile rats (PND21-22) (Reincke & Hanganu-Opatz, 2017). A more intensive maternal separation paradigm (4h/day, PND2-20)

reduces the number of PV interneurons in the mPFC in adolescent male (PND40, PND55) but not female rats (Grassi-Oliveira *et al.*, 2016). The same group demonstrated that maternal separation increased the intensity of PNN surrounding PV interneurons in the PL mPFC of adult male but not female offspring (Gildawie *et al.*, 2020). Previous studies from our laboratory have also found that LB conditions increase spine densities, evoked synaptic responses, synaptic plasticity, and the proportion of PNN surrounding PV interneurons in the BLA of male offspring exclusively (Guadagno *et al.*, 2018b; Guadagno *et al.*, 2020). We therefore include both male and female offspring in the current project to test if ELS exerts sex-dependent effects on the fear-induced responses in the mPFC.

Development of fear-related behaviors

Fear can be evoked by stimuli that are associated with aversive events through Pavlovian fear conditioning in rodents (Tovote *et al.*, 2015). In this paradigm, a particular cue (tone, odour, light) and/or context is presented together with an unconditioned aversive stimulus (US, foot shock), resulting in freezing behavior. Marked fear-conditioning emerges during late neonatal life (PND16-18) and reaches adult-like levels by the juvenile period (PND23-27) (Barnet & Hunt, 2006; Jovanovic *et al.*, 2013; Guadagno *et al.*, 2021). Fear memories can be consolidated over time, and their retrieval can be induced by presenting the conditioned cue alone in a novel context or by re-exposure to the conditioned context (Orsini & Maren, 2012). Repeated presentations of the conditioning stimulus (CS) alone without aversive events reduce fear expression, which reflects another leaning process termed extinction (Myers & Davis, 2007). From juvenility (PND21), extinguished fear memories can be reinstated by presenting a single unconditioned stimulus alone in the context in which extinction occurred or can be renewed by presenting the CS in either a novel context or the conditioning context (Tovote *et al.*, 2015; Guadagno *et al.*, 2021).

When compared to younger (PND23-27) and older animals, the expression of contextual fear is profoundly attenuated in pre-adolescent mice (PND29-33), with a lesser extent of attenuation in early adolescents (PND35-39) (PND49-70) (Pattwell *et al.*, 2011). Similarly, extinction learning is also selectively attenuated in pre-adolescents (PND29) (Pattwell *et al.*, 2012), suggesting that the fear circuitry is still maturing before puberty and may be sensitive to early adversities. Indeed, ELS exposure has been documented to enhance freezing behavior in neonatal period (PND18) and in adulthood, but not in pre-adolescence (PND28-29), and fear expression is even attenuated by ELS in late adolescence (PND45) (Arp *et al.*, 2016; Guadagno *et al.*, 2018b; Junod *et al.*, 2019; Guadagno *et al.*, 2020).

The medial prefrontal cortex in the fear circuit

The mPFC is thought to be a central hub receiving afferents from the BLA and vHP that integrate sensory inputs and present affective valence as well as contextual information (Giustino & Maren, 2015). The mPFC is also important for local processing and consolidation of emotional memories, exerting high-order control over the limbic structures to regulate adaptive behavioral responses (Marek *et al.*, 2019). There are neuroanatomically and functionally distinct subregions in the mPFC, including the prelimbic (PL) mPFC (or dmPFC) and infralimbic (IL) mPFC (or vmPFC) in rodents (Hoover & Vertes, 2007). A simplified illustration of fear circuit can be observed in Figure1. The amygdala and the prefrontal cortex are highly interconnected (Yizhar & Klavir, 2018), and their connectivity is regulated by the vHIP that innervates both structures (Tovote *et al.*, 2015). The expression of freezing behavior is mediated by the central amygdala (CeA), the main output structure of the amygdala complex (Paré *et al.*, 2004; Marek *et al.*, 2019). The conditioned cue activates PL-BLA projections or IL-BLA projections during fear acquisition and fear extinction, respectively, enhancing or suppressing the activity in the CeA (Marek *et al.*,

2019). The IL-BLA projection driven feedforward inhibition to the CeA is thought to be mediated by the medial intercalated cells (mITCs), an inhibitory cell cluster located between the BLA and the CeA (Marowsky *et al.*, 2005; Strobel *et al.*, 2015; An *et al.*, 2017).

The mPFC and the projections targeting this region mature relatively late in the developmental trajectory, making them adaptive to environmental cues but vulnerable to early adversity during critical periods (Drzewiecki & Juraska, 2020; Tottenham, 2020). The development of the mPFC starts at about embryonic day 7 and extends in adolescence (Chini & Hanganu-Opatz, 2021). The volume of the mPFC reaches its maximum at PND14, followed by a decrease at PND18, a second peak at PND24, and a gradual decrease through PND30 into adulthood, with a more pronounced volume decline in females than in males (Van Eden & Uylings, 1985; Markham *et al.*, 2007). The changes in the mPFC volume are associated with the maturation of dendritic spines in this region. In the PL, the spine density increases from juvenility to early adolescence and then declines from late adolescence until adulthood, but these patterns are not observed in the IL (Pattwell *et al.*, 2016). Our laboratory has recently shown that ELS exposure reduces functional connectivity between the BLA and the mPFC in juvenile and adult male rats and this effect appears more pronounced in the right vs left hemisphere (Guadagno *et al.*, 2018a). ELS might alter the development of glutamatergic projections between both structures, modify their activity and have local effects to regulate the excitatory/inhibitory balance in the mPFC. Currently, we do not know how ELS modifies glutamatergic inputs projecting to the mPFC in early adolescent rats and the potential consequences of altered glutamate release in this region during and after fear conditioning.

The prelimbic and infralimbic prefrontal cortex

The PL and IL cortex are neighboring structures in the mPFC, with the PL located dorsal to the IL and having relatively larger volume (Paxinos & Watson, 2005). These two regions can be distinguished anatomically based on laminar organization. Layers 2/3 appear broader and more distinct from layers 5/6 in the PL compared to the IL (Giustino & Maren, 2015) as shown in Figure 2. There are anatomical connections between the PL and IL mPFC, with major excitatory projections from layers 5/6 of PL to the same layers of IL and minor inhibitory projections from the IL to PL (Ji & Neugebauer, 2012; Marek *et al.*, 2018b). The PL and the IL mPFC receive afferents from separate subgroups of BLA projecting neurons and send their efferent back to glutamatergic neurons in the BLA that project to the CeA and the mITC, respectively (Marek *et al.*, 2019). Functionally, the PL and IL appear to exert primarily opposite effects on the regulation of fear. The PL activity is correlated with enhanced fear expression and extinction failure (Vidal-Gonzalez *et al.*, 2006; Burgos-Robles *et al.*, 2009; Sierra-Mercado *et al.*, 2011), but it is not required for the acquisition of conditioned fear (Corcoran & Quirk, 2007; Lee & Choi, 2012). In contrast, the IL activity is correlated with suppressed fear expression, successful extinction (Milad & Quirk, 2002; Vidal-Gonzalez *et al.*, 2006; Sierra-Mercado *et al.*, 2011) , and is necessary for the formation of extinction memory (Sierra-Mercado *et al.*, 2011; Do-Monte *et al.*, 2015). Neuronal activity in the PL returns to baseline soon after conditioning despite sustained fear expression, while a subgroup of IL neurons is persistently suppressed during the recovery period after fear conditioning, suggesting that suppression of IL activity might also participate in the expression of fear (Fitzgerald *et al.*, 2015). Interestingly, optogenetic activation of the projections from the PL to IL enhances fear extinction, redefining the role of the PL mPFC in fear regulation (Marek *et al.*, 2018a) and suggesting that PL and IL may also work concomitantly under some conditions.

In terms of fear learning, it has been shown that fear conditioning increases excitatory

synaptic transmission in the PL of juveniles and adults, but not pre-adolescents, while extinction training recapitulates the same age-specific effects in the IL (Pattwell *et al.*, 2012). The protracted development of the mPFC brings up the possibility that the consequences of ELS exposure on this region in adolescent animals could be distinct from adults. In fact, it was shown that ELS reduces the dendritic length and spine density in the PL mPFC in young adults, but leaves the density of dendritic spines intact in early adolescents (Monroy *et al.*, 2010). In contrast, the synaptic density in the IL mPFC is increased after ELS exposure (Ovtscharoff & Braun, 2001), suggesting a region-specific effect of ELS in the mPFC. A recent study has shown an increased neuronal activation after associative fear memory retrieval in the PL mPFC of late adolescents exposed to ELS, but not in the IL (Junod *et al.*, 2019).

Connectivity between the basolateral amygdala and the medial prefrontal cortex

There are robust structural and functional reciprocal connections between the BLA and mPFC, forming a critical bidirectional pathway for the acquisition, expression, and extinction of conditioned fear (Yizhar & Klavir, 2018). BLA projections to the mPFC preferentially synapse on cortico-amygdala neurons over neighboring corticocortical or corticostriatal neurons, laying the synaptic foundation for the strong reciprocal BLA-mPFC connectivity (Little & Carter, 2013; Anastasiades & Carter, 2021). There are significant sub-regional differences in the mPFC structures receiving BLA afferents, with more projections targeting layer 2 of the PL but more inputs to layer 5 of the IL compared to other layers in these regions (Cheriyan *et al.*, 2016; Anastasiades & Carter, 2021). Separate cell groups in the BLA are active during fear expression and extinction, termed “fear on” and “fear off” cells, respectively, that are differentially connected with the PL and the IL mPFC, encoding “high fear” and “low fear” states (Herry *et al.*, 2008; Senn *et al.*, 2014). For instance, optogenetic activation of the BLA-PL mPFC input is necessary and

sufficient to promote freezing behavior during aversive cue exposures (Burgos-Robles *et al.*, 2017).

The development of BLA projections targeting the mPFC starts from PND6, reaching a bilaminar distribution pattern seen in adults in layer2/3 and layer5/6 of the mPFC by PND16 (Verwer *et al.*, 1996; Cunningham *et al.*, 2002). The density of neurons projecting from the BLA to the PL mPFC increases from juvenile period through preadolescence (PND23–30) and followed by a subsequent decline in late adolescence (PND45) (Pattwell *et al.,* 2016). In the same study, afferents from the BLA to the IL mPFC do not show similar developmental changes, where the density of BLA-IL projecting neurons remains comparable levels between PND23-45. Functional BLA afferents to the PL mPFC are observed by PND30 and reach full maturity in adulthood, evidenced by the age-dependent prefrontal local field potential responses to BLA stimulations (Caballero *et al.*, 2014b). Given the protracted maturation of the connectivity between the BLA and mPFC, it is not surprising that the resting-state functional connectivity between these two structures is altered in animals exposed to ELS (Guadagno *et al.*, 2018a).

Ventral hippocampal afferents to the medial prefrontal cortex

The ventral hippocampal inputs to the mPFC provide contextual information in the fear circuit. Projections arise from CA1 and the subiculum and target preferentially the layer 5 in the IL mPFC, followed by layer 2/3 in IL and layer 5 in PL mPFC (Liu & Carter, 2018; Anastasiades & Carter, 2021). In general, stimulation of vHIP inputs to the mPFC exerts inhibitory control over BLA excitatory drive in this area (Thomases *et al.*, 2014). Activation of vHIP projections to the IL primarily targets interneurons and thus induces feedforward inhibition on IL pyramidal neurons, leading to extinction failure (Marek *et al.*, 2018a). Similarly, inactivation of vHIP decreases

activity of interneurons in the PL, resulting in enhanced fear expression and impaired fear extinction (Hugues & Garcia, 2007; Sotres-Bayon *et al.*, 2012). Interestingly, stimulation of vHIP-BLA afferents preferentially activate PL-projecting BLA neurons rather than IL-projecting BLA neurons to induce fear behavior (Herry *et al.*, 2008). The vHIP inputs to BLA also recruit local interneurons to drive feedforward inhibition on the BLA-mPFC projections (Hübner *et al.*, 2014).

The vHIP afferents to the PL, but not IL mPFC increases between PND23-30 before a decline in late adolescence (PND45) and adulthood (Pattwell *et al.*, 2016). The vHIP inputs into the mPFC functionally mature relatively late by PND55 and primarily serve to depress the activity of the mPFC via local GABAergic transmission (Caballero *et al.*, 2014b). Considering the protracted functional maturation of inhibitory regulation in the mPFC originating from the vHIP, it could be speculated that the early emerging vHIP afferents primarily target pyramidal neurons in the mPFC, and then vHIP-driven inhibitory innervations develop and gradually dominate in this region as excitatory synapses are pruned (Zimmermann *et al.*, 2019). Similar to BLA afferents, early stress exposure alters resting state functional connectivity between the vHIP and the mPFC later in adulthood (White *et al.*, 2020).

Local inhibitory circuits in the medial prefrontal cortex

The long-range excitatory inputs to the mPFC from the BLA, vHIP and other regions are highly regulated by local inhibitory microcircuits in this region, even though GABAergic interneurons represent a minority (10%-15% in rodents) compared with the number of excitatory pyramidal neurons in the neocortex (Tremblay *et al.*, 2016). There are primarily three largely non-overlapping populations of interneurons in the mPFC, characterized by their distinct expressions of calcium binding proteins or neuropeptides, parvalbumin (PV), somatostatin (SST), and

vasoactive intestinal peptide (VIP) (Rudy *et al.*, 2011). Together, these interneurons account for around 80% of GABAergic inhibitory neurons in the mPFC (Rudy *et al.*, 2011). Inhibitory connections in the mPFC display target-specific patterns of innervation onto neighboring neurons (Tremblay *et al.*, 2016; Anastasiades & Carter, 2021). For example, PV interneurons preferentially inhibit the peri-somatic region of nearby pyramidal neurons (soma, proximal dendrites, and axon initial segment), SST interneurons primarily synapse on the dendrites, whereas VIP interneurons target other classes of interneurons (PV and SST). In addition, PV and SST interneurons also display inhibitory innervations onto neighboring interneurons and participate in the disinhibitory gating of neuronal activity (Spampanato *et al.*, 2011).

Activation of prefrontal inhibitory interneurons in fear learning

Given the diversity of interneuron subpopulations in the mPFC, fear-related activity and plasticity of pyramidal neurons in this region are likely differentially regulated by different classes of interneurons. In fact, distinct levels of stimulation are required to activate PV and SST interneurons. A single burst of stimulation is sufficient to excite fast-spiking PV interneurons, allowing their precise and activity-dependent regulation on targeted neurons, while SST interneurons require repeated stimulations, generating prolonged but temporally delayed inhibition (Lucas & Clem, 2018). During associative fear acquisition, auditory cues suppress PV interneurons in the dorsal medial PFC to disinhibit prefrontal pyramidal neurons projecting to the BLA, leading to fear expression (Courtin *et al.*, 2014). In the same study, optogenetic inhibition of the prefrontal PV interneurons is sufficient to induce freezing behavior even in unconditioned animals. Recently, it has been shown that the activation of prelimbic SST interneurons mediates both fear memory formation and expression through inhibition of local PV interneurons (Cummings & Clem, 2020). In terms of functional integration with afferents targeting the mPFC, BLA inputs preferentially

synapse on SST interneurons rather than PV interneurons in the PL to promote fear expression via disinhibition (Cummings & Clem, 2020), whereas vHIP inputs primarily recruit PV interneurons in this region to attenuate BLA-driven fear expression via feedforward inhibition (Sotres-Bayon *et al.*, 2012). In the IL mPFC, vHIP inputs drive feedforward inhibition on to the BLA projecting neurons via PV interneurons to impair fear extinction and promote fear relapse (Marek et al. 2018a). This evidence suggests that the PV interneurons in the mPFC are recruited in both pathways of fear expression and extinction that are regulated by BLA and vHP afferents. Our current project focuses on the fear induced activities of PV interneurons in the mPFC.

Vulnerability and development of parvalbumin interneurons

The PV inhibitory interneurons express the calcium binding protein parvalbumin, which binds to presynaptic calcium ions and thus attenuates the calcium-induced potassium conductance responsible for post-spike hyperpolarization (Caillard *et al.*, 2000; Ruden *et al.*, 2021). The function of parvalbumin may in part explain the burst-firing characteristic of PV interneurons (Hu *et al.*, 2014). Meanwhile, fast-spiking action potentials require extraordinary energy that is supplied by a high density of mitochondria, rendering PV interneurons more sensitive to oxidative stress than other classes of interneurons (Ruden *et al.*, 2021).

The characteristics of interneuron types are predetermined when the progenitors leave the cell cycle (Wonders & Anderson, 2006). For this reason, if the appropriate coordination of cell-intrinsic factors and extrinsic signals is disrupted during cell migration, the prospective PV interneurons will end up in wrong places (Ruden *et al.*, 2021). When they manage to reach their ultimate destination, PV interneurons establish synaptic connections with local neurons (Hu *et al.*, 2017). The appearance of PV positive interneurons in the rat is observed relatively late from

PND10-14 in the neocortex (del Río *et al.*, 1994), and then reaches adult-like number in the mPFC by PND24 (Baker *et al.*, 2017), coinciding with the onset of critical periods of cortical plasticity (Hensch, 2005). Cortical oscillation has been studied to examine the functionality of local neuronal circuit as it reflects the level of circuit plasticity and the state of ongoing network dynamics (Reh *et al.*, 2020). The fast-spiking characteristic of PV interneurons (40Hz) makes their activity crucial for the generation of cortical gamma oscillations (30-80Hz) (Sohal *et al.*, 2009). The development of prefrontal gamma oscillation is highly correlated with the expression of PV interneurons, as fast oscillatory activity in the prefrontal cortex emerges from the second postnatal week at 15Hz and accelerates to adult-like level within gamma oscillation band by the fourth postnatal week (Bitzenhofer *et al.*, 2020). The inhibitory tone in the mPFC increases across adolescence (Thomases *et al.*, 2013; Caballero & Tseng, 2016), as evidenced by an increase in the PV protein expression and in the excitatory drive onto PV interneurons from early adolescence (PND25-35) to late adolescence (PND45-55) (Caballero *et al.*, 2014a). Interestingly, the protracted maturation of PV interneurons and their functional circuit network in the mPFC is associated with the formation of lattice-like structures in the extracellular matrix called perineuronal nets (PNNs) (Guadagno *et al.*, 2021) that have been shown to terminate critical periods of plasticity by stabilizing neuronal inputs on these interneurons.

Perineuronal nets and parvalbumin interneuron maturation

PNNs consist of large molecular aggregates composed primarily of chondroitin sulfate proteoglycans and extracellular matrix components such as collagen, laminin and fibronectin (Guadagno *et al.*, 2021). PNNs preferentially enwrap the peri-somatic region and proximal dendrites of mature PV interneurons in the mPFC (Celio *et al.*, 1998). The presence of PNNs enhances the expression of PV and stabilizes synaptic inputs onto PV interneurons as well as

gamma oscillation in this region (Carceller *et al.*, 2020), possibly because PNNs can protect PV interneurons from oxidative stress (Cabungcal *et al.*, 2013). In both PL and IL regions of the mPFC, the number of PNN positive cells increases dramatically across development from juvenility (PND24) to early adolescence (PND35-36) (Baker *et al.*, 2017), coinciding with the maturation of prefrontal PV interneurons (Caballero & Tseng, 2016) and the closure of the critical periods of synaptic plasticity (Guadagno *et al.*, 2021). In addition, degradation of PNNs or downregulation of PV expression in the PL mPFC impairs the formation of extinction memory (Hylin *et al.*, 2013; Caballero *et al.*, 2020), suggesting that PNNs might also contribute to fear regulation through modulating the maturational status of PV interneurons in the mPFC.

The unique vulnerable characteristics of PV interneurons and the relatively long developmental trajectory of these cells might make them more susceptible to environmental stressors during the late postnatal and juvenile period. Considering the correlation between the formation of PNNs and the maturation of PV interneurons, the potential consequences of ELS on the synaptic connectivity and functionality of PV interneurons might also involve effects on PNN structure and/or density. Our laboratory has recently shown that ELS exposure increases PNN density particularly around PV interneurons in parallel with impaired fear-induced activation of these cells in the BLA (Guadagno *et al.*, 2020). With a two-hit adversity model consisting of maternal separation from PND2-20 and juvenile social separation from PND21-35, (Gildawie *et al.*, 2021) found a reduction in the cell density of PV as well as PNN surrounding PV interneurons in the mPFC of adult rats, but it remains largely uninvestigated how ELS, in the form of LB conditions, might modify prefrontal PNN and/or PV expression and fear-induced activity of PV interneurons in this region in pre-adolescent rats.

B. Aims and Objectives

The neuronal circuitry that regulates fear acquisition, expression, and extinction establishes and matures during critical periods of early development and adolescence. The medial prefrontal cortex is one of the three key corticolimbic structures that constitute the fear circuit. It receives glutamatergic afferents from subcortical regions and gates the excitatory input by local inhibitory microcircuits. The protracted maturation of the projections to the mPFC and synaptic inputs onto local PV inhibitory interneurons makes this structure sensitive to early environmental challenges. Our laboratory has previously shown that ELS enhances synaptic plasticity of pyramidal neurons and maturation of PNNs around PV interneurons in the BLA of pre-adolescent offspring, and it reduces the functional connectivity between BLA and mPFC. These effects of ELS on the BLA may also lead to alterations in the development of prefrontal circuit connectivity and behavioral fear regulation. While morphological changes in pyramidal cells in the mPFC have been documented after ELS, the functional consequences of early adversity on glutamate neurotransmission in this region during fear conditioning in pre-adolescents remains unclear. The goals of this project are to examine whether ELS exposure alters fear-induced glutamatergic neurotransmission and activity of PV interneurons in the mPFC of pre-adolescent rats and whether that latter is associated with ELS-related modifications in the formation of PNNs around PV cells.

Aim1: Does ELS exposure alter glutamate release during fear conditioning in the mPFC of pre-adolescent offspring?

The first aim of this project is to test whether ELS exposure alters glutamate response to fear conditioning in the PL/IL mPFC of pre-adolescent offspring and whether the effects of ELS are age-, sex-, and subregion-dependent. To this end, we used in vivo microdialysis and high-

performance liquid chromatography to collect and quantify the extracellular glutamate concentrations in either the PL or the IL region of the mPFC before, during and after fear conditioning in pre-adolescent male, pre-adolescent female, and adult male rats. The freezing behavior was video recorded simultaneously. We were interested in the effects of ELS on both the PL and IL subregions of the mPFC as these regions primarily play opposite roles in fear regulation and might be differentially modified by ELS exposure. We hypothesize that ELS-exposed male pre-adolescent and adult offspring will show enhanced glutamate response to fear conditioning in the PL mPFC, but not in the IL mPFC, compared to the offspring reared in normal conditions and female offspring exposed to ELS.

Aim2: Does ELS exposure alter the fear-induced activity of PV interneurons in the mPFC of pre-adolescent offspring?

The second aim of this project is to test whether ELS exposure alters the activity of PV interneurons in the PL and IL mPFC during fear conditioning in pre-adolescent male and female rats, and to determine whether the formation of PNNs around these cells is also modified by ELS. To achieve this, we collected the brains of pre-adolescent male and female rats from either normal or LB rearing conditions 1 h after the onset of testing with or without fear conditioning. We quantified the cell density of activated PV interneurons as well as those PV cells surrounded by PNNs in the mPFC of these brain sections by triple fluorescence immunostainings of c-Fos, PV, and PNN. We focused on the PV interneurons as they are the most abundant class of interneurons in the mPFC and are recruited in during fear regulation. We were interested in the density of PV interneurons surrounded by PNNs because the expression of PNNs reflects the maturational status of these cells. We hypothesize that ELS exposure will impair PNN formation around PV cells in the mPFC and attenuate the fear-induced suppression of PV inhibitory interneurons exclusively in

the PL cortex of pre-adolescent male, but not female offspring.

C. Materials and Methods

Animals:

Timed-pregnant (gestation day 14) Sprague Dawley female rats (Charles River) were individually housed under controlled conditions of light (reverse cycle, 9 AM off; 9 PM on), temperature (22ºC-24ºC), and humidity (70%-80%), and provided ad libitum access to food and water. The day of parturition was considered as postnatal day (PND) 0, and litters were culled to 10 pups on PND1. Animals were weaned and group housed by sex on PND21. All experimental procedures were reviewed and approved by the Animal Care Committee at McGill University in accordance with the ethical guidelines from the Canadian Council on Animal Care.

Limited bedding paradigm:

To induce early chronic stress in the offspring, we used the limited bedding (LB) and nesting protocol adapted from Baram and colleagues (Molet *et al.*, 2014; Walker *et al.*, 2017). On PND1, dams and their offspring were randomly assigned to normal bedding (NB) or the LB condition. In the LB condition, mothers and their litters were placed on a metal mesh platform raised 2.5cm above the cage floor and thus elevated from the woodchip bedding on the floor. The mothers were given one-half piece of paper towel as nesting material. The NB cages were given approximately 2 cm layer of woodchips and one piece of paper towel. On PND10, all cages were returned to the NB condition. Mothers and litters were weighed on PND4, PND10, PND14, and PND21 when cages were changed. Maternal behavior (active/passive nursing, pup grooming, self-

grooming, eating, drinking, wandering, tail chasing) was recorded during 24 h from PND5 9 AM to PND6 9 AM using four 60 min observation sessions (two sessions in the dark phase, and two sessions in the light phase). Behavior was scored at one-minute intervals during each observation session. Fragmentation of maternal behavior was recorded when behaviors changed from one minute to the next. A total of 20 mothers and their litters (12 each bedding condition) were used in this study. A cohort of 16 dams were used for *in vivo* microdialysis experiments and another cohort of 4 dams were used for immunohistochemistry experiments.

Surgery

The surgeries for microdialysis guide cannula implantation were performed on PND23-25 in pre-adolescent male and female rats and on PND61-62 in adult male rats. Isoflurane (2%-4%) anesthetized animals were stereotaxically implanted with a 22-gauge stainless steel guide cannula (Plastics One) into either the right PL mPFC or the right IL mPFC at the following flat skull coordinates from the Paxinos atlas (Paxinos & Watson, 2005): PL pre-adolescents: anteroposterior (A/P) +2.8mm anterior to bregma, lateral (L) +0.51mm right to the midline, and dorsoventral (D/V) 2.3mm below the skull surface; PL adults: A/P 3.1mm anterior to bregma, L +0.6mm right to the midline, and D/V 2.5mm below the skull surface; IL pre-adolescents: A/P 2.8mm anterior to bregma, L +0.51mm right to the midline, D/V 2.6mm below the skull surface. We focused on the right mPFC because previous studies from our laboratory have shown that the effects of LB on the synaptic plasticity of BLA neurons and the resting-state BLA-mPFC functional connectivity were more pronounced in the right hemisphere (Guadagno *et al.* 2020, Guadagno *et al.*, 2018a). The cannula would serve to insert a microdialysis probe into the mPFC target site. The cannula was secured with acrylic dental cement anchored by two screws threaded into the cranium, with one anterior and left to bregma, and another posterior and right to bregma. An obturator extending

2.7 mm beyond the bottom tip of the cannula was inserted to prevent infection, cerebrospinal fluid (CSF) seepage, and to accommodate the probe on the experimental day. The incision was sutured with surgical silk. Animals were injected s.c. with 0.5 ml of 0.9% saline and 0.05 ml of carprofen for post-operative analgesia. All animals were allowed a minimum of 5 days of recovery before testing.

Microdialysis probes:

We used home-made I-shaped microdialysis probes (Luczynski *et al.*, 2015) comprised of side-by-side fused quartz inlet and outlet (internal diameter [ID] 50 um) wrapped in polyethylene tubing (ID 0.58-0.38mm). A regenerated, hollow cellulose membrane (Spectrum, molecular weight cut-off 13 kD; OD 216 um; ID 200 um) was secured to the end of a stainless-steel cannula (26 gauge) using cyanoacrylate adhesive and was sealed at its tip with Epoxy. The length of the active membrane was 1.5 mm. On the day of testing, the probe was inserted into the guide canula, and the probe assembly was attached to a stainless-steel spring was connected to a liquid swivel (CMA Microdialysis). A computer-controlled microdialysis pump (CMA Microdialysis) was used to pump artificial CSF (aCSF) through the probes during microdialysis. The dialysate was collected from the quartz outlet. The dead volume of the microinfusion system was approximately 5ul.

In vivo microdialysis:

In vivo microdialysis was performed on PND28-32 in pre-adolescent males and females and on PND67-70 in adult male rats. Testing took place in fear conditioning chambers (Actimetrics) in semi-dark conditions to respect the reverse light:dark cycle and a red lamp was placed on top of the cage to allow for video recordings of freezing behavior during testing. The

fear chamber was cleaned with Peroxyguard between trials. Animals were habituated to the fear conditioning chambers without cues or stimuli for 10 min per day and consecutive 2 days before testing. On the day of testing, a microdialysis probe was inserted into the animals' pre-implanted guide cannula and perfused with sterile, degassed aCSF (26 mM $NaHCO_3$, 3 mM NaH_2PO_4, 1.3 mM $MgCl_2$, 2.3 mM $CaCl_2$, 3.0 mM KCl, 126 mM NaCl, 0.2 mM L-ascorbic acid, pH=7.2) at a constant flow rate of 1ul/min. Dialysate samples were collected but discarded during the first hour of testing to habituate the animals to the microdialysis context and the presence of the experimenter. Samples were collected every 10 min before (60 min baseline), during (40 min) and after (80 min recovery) the exposure to a 40 min session of fear conditioning. During fear conditioning, animals were exposed to ten tone (50dB, 30 sec)-shock pairings (0.5sec, shock of 0.5mA, co-terminating with the tone) with an average of 4 min variable inter-trial interval (Figure 3). Dialysate samples of 10 ul were collected in microtubes containing 1ul of 0.125 M perchloric acid to prevent analyte degradation, and then were immediately frozen at -80oC prior to HPLC analysis. Freezing behavior was video recorded before, during, and after fear conditioning. The animals' behavior during the tones and inter-trial intervals of fear conditioning was manually scored and converted to percentage of freezing time. The behavior during baseline and recovery was scored from program recorded motion index (FreezeFrame software version 5, Actimetrics). The threshold of motion was determined as the program scored freezing percentage during fear conditioning was aligned to manual scoring. Freezing was defined as the absence of movement, except for respiration (Stevenson *et al.*, 2009). All animals were sacrificed at the end of the microdialysis session and brains were extracted for histological identification of probe placement.

Histology:

Microdialysis probe placements were confirmed from 20 um coronal brain sections stained

with cresyl violet. Only animals with correct placement in either the IL or PL mPFC were included in the analysis. The total number of animals were PL placement:30 pre-adolescent males and 23 pre-adolescent females, as well as 25 adult males; IL placement: 16 pre-adolescent males.

Detection of glutamate concentrations by high performance liquid chromatography:

The extracellular levels of glutamate in the dialysates were quantified by high-performance liquid chromatography with fluorescence detection (HPLC-FD) as previously described (Luczynski *et al.*, 2015). The chromatographic system was composed of a pump (UltiMate 3000 RS Pump, Dionex) and an injector connected to an Xterra MS C18 3.0mm x 50 mm, 5 um analytical column (Waters Corp.) The mobile phase consisted of 3.5% acetonitrile, 15% methanol, and 100 mMNa_2HPO_4 and was adjusted to a pH of 6.7. The flow rate was set at 0.5ml/min, and the fluorescence detector (UltiMate 3000 Fluorescence Detector, Dionex) was set to an excitation frequency of 323 nm and to an emission frequency of 455 nm.

On the day of the HPLC assay, the dialysate samples were transferred to fraction vials on ice. Working standards (100 ng/ml glutamate) and derivatization reagents were prepared freshly and loaded with the samples into a refrigerated (10ºC) autosampler (UltiMate 3000 RS Autosampler, Dionex). The reagents were refilled every 48 h until the end of a run. Before being injected into the analytical column, each fraction was sequentially mixed with 20 ul of o-phthaldehyde (OPA,2.85mM) diluted with 0.1 M sodium tetraborate and 20 ul of 3-mercaptopropionic acid (3-MPA, 75mM) diluted with H_2O and left to react for 5 min. After each injection, the injection loop was flushed with 20% methanol to prevent contamination of subsequent samples. Under these conditions, the retention time for glutamate was approximately 0.7 min, with a total run time of 24 min/sample. Chromatographic peak analysis was performed

by identification of unknown peaks in a sample according to retention times from known standards (Chromeleon Chromatography Data System software version 7, ThermoFisher Scientific). The glutamate concentrations in the samples collected from each animal tested during and after fear conditioning were converted to percentage relative to the corresponding pooled average of the six baseline samples.

Activation of parvalbumin interneurons after fear conditioning:

In order to determine whether activation of prefrontal parvalbumin (PV) interneurons after fear conditioning was altered by early life stress, we collected brain tissues of pre-adolescent pups 60 min after the onset of a fear conditioning session. All tests were performed in semi-dark conditions under red light and the testing chamber was cleaned with Peroxyguard between trials. Forty male or female pre-adolescents (PND28-29) from either NB or LB mothers were subjected to fear group or control (n=5 animals/bedding, sex, and fear conditioning treatment) on the day of testing. In fear group, animals were given 30 min to acclimatize to the experimental context before the onset of testing. Animals were habituated to the testing chamber for 5 min, and then were exposed to two habituation tones (80dB, 30sec) alone, followed by 6 tone-shock pairings (1 sec, shock of 0.6 mA, co-terminating with the tone) with an average of 2 min variable inter-trial intervals. In control group, animals were placed in the chamber for the same total duration as the fear animals but were not exposed to the tones or shocks. Sixty minutes after the onset of testing, animals were anesthetized with ketamine-xylazine (0.1 ml/100 g body weight, s.c. injection) and trans-cardially perfused with ice-cold 0.9% saline for 5 min, followed by a 20 min perfusion with 4% paraformaldehyde (PFA). The brains were extracted and stored in 4% PFA at 4^{o}C overnight, then transferred to a 30% sucrose solution in 1 X phosphate-buffered saline (PBS) for 48 h at 4^{o}C. The right side of the brains was marked using a blade, and brains were stored at -80^{o}C until slicing.

Free-floating 50 um coronal sections were stored at -20ºC in cryoprotectant solution (5.7 mM $NaH_2PO_4 \cdot H_2O$, 19.2 mM Na_2HPO_4, 30% ethylene glycol, 20% glycerol) until being processed for immunostaining.

Triple fluorescence immunohistochemistry for Fos, PV and PNN in the mPFC:

In order to examine whether fear-induced activity of PV interneurons was modified by early life experience and whether PV interneurons engulfed by perineuronal nets (PNNs) reacted differently, we performed triple fluorescence immunohistochemistry for Fos, PV and PNN on sections of both PL and IL mPFC as previously described (Guadagno *et al.*, 2020). Fifty um free floating sections were brought to room temperature for 30 min and then were washed 3 x 5 min in 1X PBS. They were incubated for 20 min with 0.3% H_2O_2 (30%, H1009, Sigma Millipore) in 1X PBS, then washed 3 x 5 min in 1X PBS. After 1 h incubation in blocking solution (2% Normal Horse Serum, S-2000, Vector Laboratories; 0.4% Triton X-100, Sigma Millipore; 1X PBS), sections were incubated with the primary anti-PV antibody (1:500, Polyclonal Guinea Pig antiserum, #195004, Synaptic Systems) for 45 min at room temperature followed by overnight incubation at 4ºC on a rotating platform. The following day, sections were washed 3 x 5 min 1X PBS and incubated for 2 h with the Secondary Goat Anti-Guinea Pig antibody Alexa-568 (1:500, A-11075, Invitrogen by Thermo Fisher Scientific) at room temperature. All procedures were performed in the dark since then. The sections were washed 3 x 5 min 1X PBS and then incubated with the primary anti-FOS antibody (1:500, Rabbit anti-Rat, #Sc-52, Santa Cruz Biotechnology) and the lectin Wisteria floribunda agglutinin (WFA) conjugated with Fluorescein (1:500, FL-1355, Vector Laboratories) for 45 min at room temperature, then overnight at 4ºC. WFA binds to N-acetylgalactosamine and is used to visualize PNNs (Hartig et al. 1992). The next day, sections were washed 3 x 5 min 1X PBS and then incubated with the Secondary Donkey Anti-Rabbit

antibody Alexa-647 (1:500, #711-605-152, Jackson ImmunoResearch Laboratories) for 2 h. Sections were washed 3 x 5 min 1X PBS and mounted onto charged slides using DAPI Hardset mounting medium (H-1500, Vector Laboratories). The slides were stored at 4ºC in dark until imaging.

Microscopy imaging and cell quantification:

Images of triple immunostained brain sections were taken with an Olympus BX63 fluorescence microscope. Six images of the PL or IL mPFC were taken per brain spanning bregma levels from +3.72 mm to +2.52 mm (Paxinos & Watson, 2005). The images were taken at 20x magnification, with exposure time of 8ms for DAPI, 15ms for GFP (PNN), 8ms for RFP (PV), and 90ms for FR (Fos). Counting of immunostained cells and cells expressing PNN was manually performed using QuPath software. The PL/IL mPFC was outlined with micrometers as unit of length and total counts were converted to cell density measurement in mm^2.

Statistical analysis:

All data were reported as mean (+/- SEM). Body weight data from PND1, PND4, PND10, and PND21 animals were analyzed using two-way ANOVA with bedding as a between-subject factor and day as a within-subject factor. Two-way ANOVA was also performed on maternal behavior with bedding as between subject factor and light phase as within subject factor. An unpaired two-tailed Student's t-test was used to assess bedding group differences in averaged basal glutamate levels (in the PL of pre-adolescent males, NB n=13, LB n=17; in the PL of pre-adolescent females, NB n=10, LB n=13; in the IL of pre-adolescent males, NB n=10, LB n=6; in the PL of adult males, NB n=13, LB n=12). The effects of ELS on the fear-induced glutamate response and freezing behavior were assessed using two-way ANOVA with bedding as a between-

subject factor and time as a within-subject factor. In the microdialysis data, extreme values for the baseline period that were more than +/-1.5 SD were removed (27 values out of 564) to obtain a more stable baseline. The relatively liberal exclusion approach was applied because the sample size of baseline (n=6) was small in each animal compared to the remainder of the samples (n=12). Outlier values in the fear conditioning and recovery sessions that exceeded 2 SD were excluded from the analysis. Missing and excluded outlier values in the mixed design two-way ANOVA analysis of microdialysis data were estimated using the formula $X.$ = [$rU + \beta$ (ABij) – Ai]/[($r -$ 1)($\beta -$ 1)], where r = the sample size of the group with the missing/excluded data point, U = total for the subject with the missing/excluded data point, $\beta =$ the number of levels of the within subject factor, ABij = total for all the subjects at the timepoint with the missing/excluded data point, and Ai =total for the entire group with the missing/excluded data point (Cochran & Cox, 1957). For the immunohistochemical data, the effects of ELS on the expression of FOS+, FOS+/PV+, and FOS+/PV+/PNN+ cells after fear or control testing (n=5 animals per group) were analyzed using two-way ANOVA with bedding and fear treatment as between-subject factors. The density of PV+, PNN+, and PV+/PNN+ cells were analyzed using two-way ANOVA with sex and bedding treatment as between-subject factors. Significant interactions were further assessed by simple main effects analysis, followed by post-hoc Dunnett's tests to compare the experimental timepoints against the baseline in the case of microdialysis experiments or post-hoc Bonferroni tests to compare all pairwise experimental groups in freezing behavior and immunohistochemistry data sets. The level of significance was set at $p<0.05$. Graphs were created with Prism 8 (GraphPad Software).

D. Results

Effects of limited bedding on offspring body weight and maternal behavior

To induce early life stress in the offspring, mothers and their litters were placed on either LB conditions or NB conditions between PND1-10. Pup body weight was measured on PND1, PND4, PND10, PND14, and PND21. As shown in Figure 4, LB conditions significantly reduced body weight gain of pups as two-way ANOVA revealed a significant main effect of bedding ($F(1, 14)=8.55$, $p=0.0111$), a significant main effect of age ($F(4, 56)=692.06$, $p<0.0001$), and a significant age x bedding interaction ($F(4, 56)=4.401$, $p=0.024$) on litter body weights. Simple main effect tests indicated that the significant difference between NB and LB offspring was seen on PND10 and PND21 ($F(1,62)>=7.73$, $p<=0.0075$). Maternal behavior was video recorded for 24 hours between PND5-6 and was manually scored 2 hours in the dark phase and 2 hours in the light phase. Behaviors were analyzed in terms of three main categories: nursing (both active and passive), pup grooming, and fragmentation. As shown in Figure 5, two-way ANOVA with bedding and phase of the light cycle (repeated measure) as factors were used to analyze maternal behavior. NB and LB mothers nursed more in the light than the dark phase with a significant main effect of light cycle ($F(1,14)=36.65$, $p<0.0001$), but no significant main effect of bedding ($F(1,14)=0.033$, $p=0.8575$) and no bedding x light cycle interaction ($F(1,14)=3.618$, $p=0.0779$) (Figure 5A). For the pup grooming behavior, there was no significant main effect of bedding or light (bedding effect: $F(1,14)=0.1733$, $p=0.6835$; light effect: $F(1,14)=1.345$, $p=0.2655$), and no significant bedding x light cycle interaction ($F(1,14)=0.003$, $p=0.9567$) (Figure 5B). The fragmentation of maternal behavior was similar between NB and LB mothers (main bedding effect: $F(1,14)=0.8430$, $p=0.3741$), although there was generally higher fragmentation during the dark than the light phase (main light cycle effect: $F(1,14)=64.48$, $p<0.0001$), with no significant bedding x light cycle interaction ($F(1,14)=0.843$, $p=0.3741$) (Figure 5C).

Prefrontal glutamate concentrations during fear conditioning in NB and LB offspring

To test whether ELS alters fear-induced glutamate release in the mPFC, we collected extracellular glutamate samples before, during and after a 40 min session of fear conditioning by *in vivo* microdialysis in either the PL or IL mPFC in pre-adolescent (PND28-32) or adult (PND67-70) rats. Microdialysate samples were collected every 10 min during testing and glutamate concentrations in the samples were analyzed by HPLC. Only animals with confirmed microdialysis probe placements within the PL or IL mPFC were included in the HPLC analysis. Figure 6A and 6B are the representative probe placements in the right PL and IL mPFC, respectively.

Pre-adolescents: Data are depicted in Figures 7 (PL mPFC) and 8 (IL mPFC, males only). For the PL mPFC, basal levels of glutamate concentrations averaged over 6 samples were not significantly different between NB and LB offspring of males ($t(26)=0.6912$, $p=0.4956$, Figure7A) and females ($t(21)=1.239$, $p=0.2290$, Figure7B). All values of glutamate concentrations after the onset of fear conditioning were expressed as a percentage of the average baseline concentrations. In male offspring, ANOVA analysis showed that there was a trend of bedding effect ($F(1,28)=2.45$, $p=0.1287$), but no main effect of time ($F(12, 336)=1.207$, $p=0.2766$) or time x bedding interaction ($F(12, 336)=1.262$, $p=0.2395$) on fear-induced glutamate release. Even though bedding effect did not reach significance, glutamate concentrations in the PL mPFC increased after fear conditioning in NB male rats, while this response was absent in LB male rats. Post-hoc Dunnett's tests revealed that fear conditioning significantly increased prelimbic extracellular glutamate concentrations during the first 20 min of fear conditioning (F1, F2) and the last 10 min of testing (R8) in the NB male offspring only ($p<0.05$, Figure7C). In pre-adolescent females, ANOVA analysis showed that fear-induced changes in glutamate concentrations were not affected by bedding conditions ($F(1,21)=0.393$, $p=0.5373$) or time ($F(12, 244)=0.6508$, $p=0.7972$) in the PL mPFC (Figure7D).

In addition to the lack of significant bedding effect on the fear-induced glutamate response that we observed in the PL mPFC of pre-adolescent females, our previous studies have also demonstrated that adolescent and adult fear conditioning freezing behavior was not affected by LB exposure in female offspring (Guadagno *et al*., 2018a; Guadagno *et al*., 2020). Other studies have documented that the developmental trajectory of the BLA to IL mPFC axonal innervation was altered in early adolescent males (PND28-38), but not in females (Honeycutt *et al.*, 2020). Based on these observations, we prioritized microdialysis studies in males for the IL mPFC (Figure 8), keeping the investigation of females for future studies. In the IL mPFC, baseline glutamate levels were unaltered by bedding conditions ($t(14)=0.322$, $p=0.7522$) (Fig 8A). After the onset of fear conditioning, two-way ANOVA revealed a significant main effect of time ($F(12, 168)=2.107$, $p=0.0189$), but no significant main effect of bedding ($F(1,14)=0.4413$, $p=0.5173$) and no significant time x bedding interaction ($F(12,168)=0.391$, $p=0.9653$) for glutamate concentrations in the IL mPFC (Fig 8B). Subsequent Dunnett's post-hoc tests revealed that the infralimbic glutamate concentrations were raising significantly at the end of the recovery period (R6, R7) in the NB group only ($p<0.05$).

Adults: To test whether ELS alters fear-induced glutamate response in the adults differentially from pre-adolescents, we tested adult males with probe placement in the PL mPFC (Figure 9). As for the pre-adolescent offspring, NB and LB adult males displayed similar basal levels of glutamate release in the PL mPFC ($t(22)=0.3418$, $p=0.7357$) (Figure9A). ANOVA for the fear-induced prelimbic glutamate responses in NB vs. LB adult animals showed no significant main effect of time ($F(12,264)=0.57$, $p=0.8645$), but a significant main effect of bedding ($F(1,22)=4.70$, $p=0.0358$) and time x bedding interaction ($F(12,264)=2.34$, $p=0.0074$) (Fig 9B). Simple effect tests conducted over time within bedding conditions revealed a significant effect of

time in LB adult males ($F(12,264)=2.13$, $p=0.0158$), but not in NB controls ($F(12, 264)=0.78$, $p=0.6696$). Subsequent post-hoc Dunnett's tests found that the glutamate levels significantly increased above baseline at 20 min during (F2, $p<0.05$), and at 60 min as well as 80 min after fear conditioning (R6 and R8, $p<0.05$) in the LB exposed adult offspring exclusively.

Freezing behavior during fear conditioning in NB and LB offspring

To examine whether ELS-induced alterations in the prefrontal glutamate responses to fear conditioning are associated with altered behavioral fear expression, we scored the freezing behavior during the 40 min of fear conditioning (10 tone/shock pairings) and as recovery of tone/shock pairings for the next 80 min. In pre-adolescents, we observed that freezing behavior significantly increased in both NB and LB male and female offspring (Figure 10). ANOVA showed a significant effect of time ($F(9,252)=11.09$, $p<0.001$), but no significant effect of bedding ($F(1,28)=0.945$, $p=0.3393$) or time x bedding interaction ($F(9,252)=1.260$, $p=0.2592$) in pre-adolescent males (Figure 10A). Similar effects were seen in pre-adolescent females (time effect: ($F(9,189)=9.305$, $p<0.001$); bedding effect ($F(1,21)=1.41$, $p=0.2480$); time x bedding interaction ($F(9,189)=0.9923$, $p=0.4478$) (Figure 10B). Freezing behavior in tones 3-10 was significantly elevated over the first 2 tones in male (post-hoc Bonferroni test, $p<=0.0387$) and female (post-hoc Bonferroni test, $p<=0.0276$) pre-adolescent offspring. In adult males, LB offspring displayed significantly higher fear induced freezing during tones compared to NB controls (time effect: $F(9,128)=22.75$, $p<0.0001$; bedding effect: $F(1,22)=8.961$, $p=0.0067$), with no time x bedding interaction ($F(9, 198)=0.555$, $p=0.8325$) (Figure.10C). Post-hoc Bonferroni tests revealed that in the ten tone-shock pairings, freezing behavior significantly increased after the first two tones in both groups of animals ($p<0.001$), and the LB offspring displayed significantly higher freezing at the 5^{th} and 8^{th} tone compared to NB controls ($p<=0.0489$). In addition to analyzing fear behavior

during the 30sec tone-shock pairings, we also determined whether freezing behavior was altered during the intervals between the tone/shock pairings as depicted in Figure 11. Similarly to the fear behavior recorded during conditioning tones, we observed that all groups of animals showed significantly increased freezing during the intervals across testing time (pre-adolescent male: $F(9,252)=4.37$, $p=0.0023$; pre-adolescent female: $F(9,185)=3.94$, $p=0.0073$; adult male: $F(9,198)=6.325$, $p<0.0001$). Interestingly in adult males only, freezing behavior of LB offspring remained higher than NB controls (bedding effect: $F(1,22)=5.326$, $p=0.0308$; time x bedding interaction: $F(9,198)=1.537$, $p=0.1370$), consistent with the behavior observed during the tone-shock pairings (Figure 11C). During recovery from fear conditioning, freezing significantly declined in the last ten minutes of recovery compared to the first ten minutes in both bedding groups of pre-adolescent males (time effect: $F(7,189)=2.683$, $p=0.0113$, post-hoc Bonferroni test: 10 min vs. 80 min, $p=0.0085$), with no significant effect of bedding condition ($F(1,27)=0.156$, $p=0.6964$) or time x bedding interaction ($F(7,189)=0.5339$, $p=0.8081$) (Figure 12A). There was no significant effect of time or bedding in the freezing behavior recorded during the recovery period in pre-adolescent females (time: $F(4.06, 85.3)=1.65$, $p=0.1625$; bedding: $F(1,21)=1.35$, $p=0.2588$) or adult males (time: $F(4.217,92.76)=2.137$, $p=0.0790$; bedding: $F(1,22)=0.306$, $p=0.5857$) (Figure 12B, 12C).

<u>Prefrontal neuronal activation and maturation of parvalbumin interneurons in NB and LB pre-adolescent offspring</u>

In this part of the study, we aimed to determine whether fear-related activity of inhibitory interneurons, and in particular parvalbumin interneurons is altered by early life stress conditions, which might influence glutamatergic concentrations in the mPFC. The initial part of the study determined whether LB conditions modified the number of PV interneurons and their maturation

as evidenced by the number of PV neurons harboring perineuronal nets (PNN). We studied both the PL and IL mPFC. Some of the results presented here were acquired by another member of our laboratory (PV/PNN cell density in the PL mPFC), but are mentioned here because they are relevant to our discussion. These results will be clearly indicated with ***. To measure the activation of PV interneurons after fear conditioning and their maturational status we performed triple fluorescence immunohistochemistry with cFos, PV, and PNN on brain sections collected from NB and LB PND28-29 offspring 60 min after the onset of fear conditioning or in control pre-adolescents not exposed to tone/shock pairings. As shown in Figure 13 we found false positive cFos signals colocalized with PV cells in the PL mPFC after fear conditioning. Representative images with triple immunostaining, in which cFos positive cells were shown in cyan (far red fluorescence channel), PV positive cells were shown in red (rhodamine channel), and PNN positive cells were shown in green (GFP channel). However, as illustrated in figure 13A and 13B, we had a leak through signal from the red fluorescence channel to the far-red fluorescence channel due to a deficient far-red filter on the fluorescence microscope (Olympus BX63) we used. Although we were able to quantify cFos positive cells based on their round positive signals expressed in the nucleus, which were distinct from cytoplasmic PV positive signals, co-localization of cFos and PV positive signals was not possible to be analyzed. Because of this technical issue, we will not discuss the prefrontal activation of PV interneurons, but only overall neuronal activation during fear conditioning or control conditions. In addition, these current data will allow to determine whether LB conditions modify the number of PV cells expressing PNN. Currently, we are also repeating some of these experiments using a different microscope with a better-defined signal discrimination range. Quantification of the immunohistochemical signal and cFos cell density in the PL (***) and IL mPFC is displayed in Figures 14A-B and 14 C-D, respectively.

In the PL mPFC of pre-adolescent males, the density of cFos positive cells was not significantly altered by fear conditioning ($F(1,16)=0.6904$, $p=0.4183$) or bedding ($F(1,16)=0.0252$, $p=0.8759$) and there was no interaction between testing treatments (control or fear) and bedding conditions ($F(1,16)=0.6073$, $p=0.4472$) (Figure14A***). Surprisingly, in the IL mPFC, although there was no significant effect of bedding ($F(1,15)=0.0064$, $p=0.9372$) or test condition ($F(1,15)=2.4202$, $p=0.1421$) in pre-adolescent males, fear conditioning tended to decrease the cFos expression in the NB, but not LB male offspring (post-hoc Bonferroni test $p=0.0728$) (Fig 14C). In pre-adolescent females, the differences between fear and control groups ($F(1,16)=0.0890$, $p=0.7693$) or between NB and LB rearing ($F(1,16)=2.403$, $p=0.1407$) in the density of cFos positive cells were not significant in the PL mPFC (Figure 14B***). There was no significant effect of testing ($F(1,16)=0.0038$, $p=0.9512$) or bedding condition ($F(1,16)=1.525$, $p=0.2347$) for the infralimbic cFos expression in pre-adolescent females (Figure 14D).

For the analysis of PV, PNN and PV/PNN cell density results from both control and fear-exposed offspring were pooled. ANOVA of PV cell density in the PL mPFC (Fig 19A***) showed a significant main effect of bedding ($F(1,36)=4.226$, $p=0.0471$) and a significant main effect of sex ($F(1,36)=7.479$, $p=0.0096$), but no significant bedding x sex interaction ($F(1,36)=0.0231$, $p=0.8800$). Post-hoc Bonferroni test revealed that PV expression was significantly lower in the NB males compared to females ($P=0.0486$), but the sex difference was not found in LB offspring (Figure15A, 16A, 19A***). In the IL, a significant main effect of bedding ($F(1,35)=8.648$, $p=0.0058$) but no significant main effect of sex ($F(1,35)=1.625$, $p=0.2108$) or bedding x sex interaction ($F(1,35)=0.0051$, $p=0.9437$) was observed. LB offspring expressed significantly lower PV positive cells than NB offspring in pre-adolescent females ($p=0.0378$), and the difference between bedding conditions was close to significance in males ($p=0.0531$) (Figure17A, 18A, 19B).

Analysis of PNN expression showed that there was no significant effect of bedding condition in the PL ($F(1,36)=1.366$, $p=0.2502$) or in the IL mPFC ($F(1,35)=0.061$, $p=0.8066$)). PNN cell density was significantly lower in LB males than females in the PL (sex effect: $F(1,36)=4.113$, $p=0.0500$, post-hoc Bonferroni test $p=0.0391$) (Figure 15B, 16B,19C***), whereas PNN cell density was not affected by sex in the IL mPFC of pre-adolescents ($F(1,35)=1.878$, $p=0.8066$) (Figure 17B, 18B, 19D).

To examine whether ELS alters PNN formation around PV interneurons in the mPFC, we quantified the co-expression of PV and PNN in the PL and IL mPFC. In the PL mPFC, ANOVA showed a significant effect of bedding condition ($F(1,36)=6.081$, $p=0.0186$) and sex ($F(1,36)=10.76$, $p=0.0023$), but no bedding x sex interaction ($F(1,36)=0.6743$, $p=0.4169$). The density of cells co-expressing PV and PNN in the PL mPFC was significantly lower in the LB males than females ($p=0.0056$), and was decreased by LB exposure in males only ($p=0.0279$) (Figure15C,16C,19E***). The density of cells co-expressing PV and PNN was also significantly altered by bedding condition in the IL mPFC of pre-adolescents ($F(1,35)=8.322$, $p=0.0067$), but no significant main effect of sex ($F(1.35)=1.927$, $p=0.1739$) and no significant bedding x sex interaction ($F(1,35)=0.6138$, $p=0.4386$) were observed. Post-hoc Bonferroni test revealed that LB exposure significantly decreased the density of PV/PNN positive cells in the IL mPFC of pre-adolescent males ($p=0.0150$), but not females (Figure 17C, 18C, 19F).

E. Discussion

It has been well documented that early adversity induces structural and functional alterations in the fear circuitry, primarily including the mPFC, the BLA, and the vHIP. In this

project, we examined the effects of early life stress, in the form of the limited bedding (LB) paradigm, on the fear-induced glutamate release in the IL and PL regions of the mPFC and on the activity as well as the maturation of PV interneurons in these regions. The early programming by ELS of subcortical inputs targeting the medial prefrontal cortex together with changes in the prefrontal local inhibitory microcircuits might exert long-term consequences on the regulation of fear acquisition and expression in offspring exposed to ELS. Glutamatergic neurotransmission and activity of parvalbumin interneurons in the mPFC during fear conditioning represent the balance between functionality of excitatory afferents projecting to this region and the recruitment of local inhibitory interneurons that regulate the activity of prefrontal principal neurons. These neurons project to several brain areas, including the amygdala, where they regulate fear extinction and fear memory and participate in behavioral regulation. In our studies, we found that LB exposure significantly enhanced fear-induced glutamatergic neurotransmission in the PL mPFC of adult males. In pre-adolescent animals, the glutamate response to fear conditioning tended to be suppressed in the PL mPFC of male, but not female offspring exposed to LB conditions, whereas the glutamate release in the IL mPFC of male offspring during fear conditioning was not affected by postnatal bedding conditions. Consistent with the fear-induced prelimbic glutamate response, freezing behavior was increased by LB conditions in adult males, but not in pre-adolescent males and females, although all groups of animals effectively acquired the fear conditioning. The acquisition of PNN as a proxy for the maturation of PV interneurons was delayed by LB conditions in both PL and IL mPFC of pre-adolescent male, but not female offspring.

Effects of LB on pup body weights and maternal behavior

Consistent with other reports (Moussaoui *et al.*, 2017; Guadagno *et al.*, 2018b; Guadagno *et al.*, 2020), LB offspring displayed a significant reduction in body weights on PND10, the end

of limited bedding treatment, and on PND21. We did not observe a significant difference in pup body weight between bedding conditions on PND14, possibly because there was one LB litter having one less pup than other litters. The LB-induced reduction in pup body weight is likely to be transient rather than long-lasting as our laboratory has previously documented that the differences in body weight between NB and LB offspring did not persist on PND28 (Guadagno *et al.*, 2020). There are several factors that may account for the reduction in pup body weight in LB conditions. Increased energy expenditure might be observed due to lower nest temperature and the virtual absence of bedding material to construct a proper nest. Alternatively, there could be a reduced nutritional intake in part dependent on maternal nursing behavior, and maternal fragmentation or a combination of both (McLaughlin *et al.*, 2016; Walker *et al.*, 2017). However, as observed in our previous studies (McLaughlin *et al.*, 2016; Guadagno *et al.*, 2018b), LB mothers displayed similar maternal behavior in terms of nursing time, pup grooming, and fragmentation compared to NB mothers, suggesting that the reduced body weights in LB pups might result from a lower rearing temperature on the metal mesh platform. Although we did not observe increased fragmentation of maternal behavior in LB conditions, the reduction in body weight indicated that chronic early life stress was induced in LB offspring. In fact, it has been documented that low pre-pubertal body weight is associated with long-term deficits of cognitive functions and emotional regulation later in life in ELS-exposed rodents and humans (Corbett & Drewett, 2004; Manzano Nieves *et al.*, 2020).

Long-lasting consequences of LB exposure on fear behavior

As expected, freezing behavior was significantly increased during fear conditioning in pre-adolescent males, pre-adolescent females, and adult males, suggesting that pre-adolescent rats (PND28-29) already display adult-like level of fear acquisition. Previous studies have indeed

documented that fear conditioned freezing behavior matures during the juvenile period (PND21-27) (Jovanovic *et al.*, 2013). The expression of freezing behavior during fear conditioning is thought to be mediated by the enhanced activity in the central amygdala (CeA) that receives excitatory inputs from the BLA (Marek *et al.*, 2019). Therefore, it is speculated that the age-related morphological and functional changes in the BLA neurons contribute to the development of freezing behavior during fear acquisition. Indeed, soma size, dendritic arborization, and the density of dendritic spines of BLA neurons reach maturity by pre-adolescence (PND28-30) (Moryś *et al.*, 1998; Ryan *et al.*, 2016). In parallel with morphological development, the electrophysiological characteristics of BLA neurons including passive membrane properties, action potential waveforms as well as long term potentiation (LTP) reach adult-like patterns during the fourth postnatal week (Ehrlich *et al.*, 2012; Ryan *et al.*, 2016; Bender *et al.*, 2017). The development of BLA neurons and synapses is associated with the increased density of reciprocal projections between the BLA and the mPFC that reaches plateau by PND 30 (Bouwmeester *et al.*, 2002; Cressman *et al.*, 2010; Pattwell *et al.*, 2016; Arruda-Carvalho *et al.*, 2017), possibly reflecting the maturation of the BLA-mPFC circuit that control over the CeA outputs and thus the expression of freezing behavior.

In the current study, we confirmed that LB exposure enhanced freezing behavior during fear conditioning in adult males, but not in pre-adolescent males and females. We focused on male offspring in adults because we previously found that the behavioral response to fear conditioning was significantly altered in adult males specifically (Guadagno *et al.*, 2018b). Interestingly, sex-differences in the effect of LB on freezing behavior was not seen in pre-adolescents, suggesting that the sex-dependent ELS effects on fear acquisition emerge after puberty. The age-dependent effects of LB conditions we observed in freezing behavior are consistent with changes in the

development of conditioned fear expression after ELS in other studies (Guadagno *et al.*, 2018b; Junod *et al.*, 2019; Guadagno *et al.*, 2020). Relative to NB controls, LB exposure enhances freezing behavior in PND18 pups, but does not alter freezing response in pre-adolescent LB offspring (PND28-29). In adolescent rats (PND45), LB was found to even attenuate fear expression before increasing freezing behavior above control level in LB adults. Considering that the maturation of BLA neurons and their connections with the mPFC are tightly linked to the development of fear expression, our behavioral results might be explained by ELS-induced developmental pattern of amygdala function rather than that of the mPFC (Junod *et al.*, 2019). Indeed, our previous study showed that LB conditions did not alter fear-induced activation of BLA neurons on PND28 offspring (Guadagno *et al.*, 2020). Other reports show that ELS exposure decreases fear-induced neuronal activation across amygdala nuclei in adolescents but increases the intrinsic excitability of BLA neurons in adults (Rau *et al.*, 2015; Junod *et al.*, 2019).

It is worth noting that the consequences of early adversity on fear expression during conditioning could be different from the ELS effects on the expression of fear memory during retrieval. For instance, ELS-exposed offspring display similar levels of freezing behavior during fear acquisition compared to NB controls, but lower freezing to the conditioned context or auditory cues on the next day of testing in both male and female adolescents (PND35) (Chocyk *et al.*, 2014). Thus, our results cannot exclude the possibility that LB exposure may alter the expression of fear extinction or fear memory in pre-adolescent rats, but we did not test for these specific modalities. The differential effects of ELS on fear learning and memory might rely on distinct corticolimbic pathways underlying fear acquisition, extinction, and retrieval. Specifically, the connectivity between amygdala and the PL mPFC is important for fear acquisition and behavioral fear expression, while both the PL and the IL mPFC are required for the retrieval of fear and the

extinction of fear respectively (Giustino & Maren, 2015; Yizhar & Klavir, 2018; Marek *et al.*, 2019).

Effects of LB conditions on fear-induced glutamatergic neurotransmission in the mPFC

The mPFC receives several glutamatergic long-range projections from various subcortical regions and other cortical areas, but it is the projections originating primarily from the BLA and the vHIP that are implicated in fear learning (Giustino & Maren, 2015). Glutamate concentrations in the mPFC measured by *in vivo* microdialysis represents a dynamic sum of all glutamatergic activated inputs reaching the specific mPFC region examined as well as local glutamatergic release by mPFC neurons. In our experiments, we targeted the microdialysis probe to the laminar L2/L3 zones of the mPFC because these laminar regions receive mostly inputs from the BLA (L2), contralateral mPFC (L2-6) and some from the mediodorsal thalamus (L3) (Anastasiades & Carter, 2021). However, the probe placements ended between L2-5 due to the relatively large size of the guide cannula. In adult males, our data showed that relative to NB controls, LB exposure in early life enhanced glutamate release in the PL mPFC during and after fear conditioning, without changes in the basal levels of glutamate concentrations. This suggests that the effects of early life adversity are only observed when the system is challenged, for instance in response to fear conditioning. As LB conditions enhance glutamatergic neurotransmission in adults, we do not know if it results from a general activation of several long-range inputs to the mPFC or whether we can narrow down the activated inputs to those originating from the BLA. Previous studies have documented that optogenetic activation of BLA-PL mPFC projections induces freezing responses (Burgos-Robles *et al.*, 2017), while stimulation of the vHIP afferents attenuates fear expression (Thomases *et al.*, 2014). Given this, we suggest that the BLA rather than the vHIP inputs might contribute to the increased glutamate response to fear conditioning observed in the PL mPFC of

LB-reared adult males, in parallel with the enhanced freezing behavior. In fact, increased structural connectivity between the amygdala and the mPFC was found in LB-exposed adult males using diffusion tensor imaging (Bolton *et al.*, 2018).

Interestingly, we did not observe a significant glutamate response to fear conditioning in NB-reared adult males, even though fear-induced behavioral responses were successfully acquired in these animals. The absence of fear-induced glutamate release in controls might be due to limitations of the *in vivo* microdialysis technique to measure total glutamate release. Since the microdialysis probe cannot get access to the synaptic cleft, glutamate molecules collected during microdialysis only represented a fraction of total glutamate molecules that escaped from glial uptake and diffused to the extra-synaptic space. These data also suggest that either the mPFC glutamate threshold to induce freezing behavior in adults is extremely low, or that other brain regions such as amygdala rather than the mPFC actively participate in the behavioral freezing response.

The upregulated fear-induced glutamatergic transmission in the prelimbic cortex of LB adult offspring might also result from altered structural and functional characteristics of the neurons and synapses in the mPFC after ELS exposure. For example, early adversity can increase LTP in the PL mPFC of adult male rats (Baudin *et al.*, 2012) and spine densities in the anterior cingulate cortex of the offspring after exposure to a prolonged paradigm of maternal separation (3h/day, PND3-21) (Muhammad & Kolb, 2011). However, other studies have also reported the opposite effects on spine density in the same region using a shorter and less severe maternal separation paradigm (1h/day, PND1-12) (Monroy *et al.*, 2010). Our current data do not include morphological analysis of the consequences of LB on mPFC and thus, do not allow to conclude on the contribution of local morphological and functional changes in the mPFC after LB

conditions. Future experiments could include Golgi analysis of mPFC neurons, specifically in L2 region of the mPFC after LB treatment.

In contrast to the adults, we found that LB exposure tended to suppress the glutamate response to fear conditioning in the PL mPFC of pre-adolescent males (PND28-32) with no changes in baseline levels of glutamate between bedding groups. The suppression of glutamate release in LB was surprising but could be explained by several factors including changes in the maturation of afferent glutamatergic projections to the pre-adolescent mPFC and local changes in regulation of glutamate extrasynaptic concentrations. Of interest in the context of a possible reduced glutamatergic neurotransmission in ELS exposed young rats is a previous report showing that pharmacological upregulation of glutamatergic transmission during juvenility and adolescence (PND25-46) could rescue ELS-induced deficits in cognitive abilities later in adulthood (O'Connor *et al.*, 2015). One possibility to explain the reduced fear-induced extracellular glutamate concentrations in LB pre-adolescent males might be an enhanced glutamate uptake in this region. Increased expression of glutamate aspartate transporter in the mPFC and hippocampus was observed in early adolescent rats (PND34) following ELS exposure (O'Connor *et al.*, 2015). However, if this was the case, one would expect to see reduced glutamate in the LB group under baseline conditions as well as fear-induced conditions. Alternatively, the effects of LB on glutamatergic transmission in the pre-adolescent PL mPFC might result from LB-induced modifications in the maturation of synaptic connections in this structure and the developmental trajectory of excitatory projections targeting this region. In LB male pre-adolescent, the pattern of glutamate response to fear conditioning in the PL mPFC was similar to that of adult NB males, suggesting perhaps that LB might accelerate the synaptic remodeling and the reorganization of glutamatergic afferents in the PL mPFC. Previous literature has documented that the surge of spine

density in the PL mPFC of normally reared animals is observed around PND30 in mice, together with a peak in afferent projections from the BLA and the vHIP (Pattwell *et al.*, 2016). We specifically chose this age period for our experiments in order to get the best sensitivity of effects. If LB leads to an accelerated maturation of the corticolimbic circuit, this might lead to a faster synaptic pruning and thus a decline in spine density as well as excitatory inputs in the PL mPFC of pre-adolescent animals (PND28-32). In these conditions, we could expect a lower glutamate release under fear conditioning. Several observations support our hypothesis as downregulation of synaptic connectivity and plasticity in the PL region has been reported in ELS-exposed young rats (Moryś *et al.*, 1998; Chocyk *et al.*, 2013; Majcher-Maślanka *et al.*, 2018). In these studies, maternal separation decreases spine density and dendritic length of the pyramidal neurons in the PL mPFC, in parallel with an impairment of LTP in this region in the early adolescent rats (PND35). The modified microglial dynamics after ELS exposure may play a role in the upregulation of synaptic pruning (Ganguly *et al.*, 2018; Johnson & Kaffman, 2018).

Exposure to unfavorable conditions in early life (LB) is likely to alter maturation of mPFC afferent inputs, in particular those originating from the BLA specifically. Indeed, our laboratory and others have previously demonstrated that the resting-state functional connectivity between the BLA and the mPFC is reduced in ELS-exposed pre-pubertal male offspring (Guadagno *et al.*, 2018a; Honeycutt *et al.*, 2020), possibly reflecting the advanced maturation of the BLA-mPFC reciprocal connections. Interestingly, advanced maturation of corticolimbic circuits has also been reported in children exposed to early adversity (VanTieghem & Tottenham, 2018). For instance, previously institutionalized children exhibit more mature amygdala-prefrontal functional connectivity during an emotional conflict task (Gee *et al.*, 2013). Despite a lower glutamate release during fear conditioning, LB pre-adolescent males displayed adult-like freezing behavior that were

indistinguishable from that of their NB counterparts. The precocious maturation of emotional circuitry following early adversity could be adaptive in the short term, but might increase the vulnerability to emotional dysregulation later in adulthood (Callaghan & Tottenham, 2016). Indeed, LB-reared adult males exhibited enhanced glutamate and freezing responses to fear conditioning compared to NB controls. Further research will be needed to investigate the consequences of LB on projection-specific contributions of the BLA and the vHIP inputs towards fear-induced glutamatergic transmission in the mPFC during pre-pubertal period.

During fear conditioning, glutamate release in the PL mPFC of pre-adolescent females and in the IL mPFC of pre-adolescent males was not altered by LB conditions, suggesting that the consequences of ELS on the fear-induced glutamatergic transmission in the mPFC are both sex- and region-dependent. There is limited available literature documenting the consequences of ELS on the PL mPFC of peri-pubertal female rats. Honeycutt *et al.*, 2020 recently demonstrated that maternal separation enhances BLA-derived axonal innervation to the PL mPFC in pre-adolescent (PND28) and late adolescent (PND48) females, but not in the same age males. The enhanced projections are accompanied with stronger resting-state functional connectivity between the BLA and the PL mPFC in the ELS-exposed late adolescent females, while the opposite has been documented in males (Guadagno *et al.*, 2018a; Honeycutt *et al.*, 2020). The strengthened structural and functional BLA-PL mPFC connectivity in females might compensate for some of the detrimental effects of ELS. Sex-dependent effects of ELS on the corticolimbic system have been well documented, with a more pronounced effect on male compared to female offspring (Walker *et al.*, 2017; Guadagno *et al.*, 2021), which is consistent with our current data. In contrast to the PL mPFC, we did not find effects of early rearing conditions on IL mPFC glutamate neurotransmission in pre-adolescent male rats. This is not necessarily unexpected as the IL is

primarily involved in fear inhibition (extinction) and recall rather than fear acquisition (Milad & Quirk, 2002; Vidal-Gonzalez *et al.*, 2006; Marek *et al.*, 2019). The region-specific effects of ELS on the mPFC might rely on the differential developmental trajectory of the prefrontal synaptic connections. Unlike the PL region, the density of dendritic spines in the IL mPFC and the density of the BLA and vHIP projections to this region do not change across the developmental period from juvenility to adulthood (Pattwell *et al.*, 2016). Accordingly, it is likely that ELS-induced alterations in the morphological characteristics of the IL neurons are different from those in the PL, with no significant change in dendritic length and spine density in the IL mPFC of adolescent males (Farrell *et al.*, 2016).

Effects of LB conditions on fear-induced neuronal activation in the mPFC

In addition to the determination of glutamatergic neurotransmission in the mPFC of pre-adolescent rats, we wanted to determine whether LB could affect mPFC overall activation under basal and fear-conditioning conditions in a sex-dependent manner. We used cFos, an immediate early gene, to measure neuronal activation in the PL and the IL mPFC of pre-adolescent offspring (PND28-29) 60 min after the onset of fear conditioning or control testing. We recognize that a unique time point provides only a snapshot of neuronal activation after fear conditioning and during recovery after fear exposure. In general, we did not observe significant effects of fear treatment or LB condition on cFos positive cell density in the PL and IL mPFC of pre-adolescent male and female offspring. The density of cFos positive cells tended to be reduced by fear conditioning in the IL mPFC of NB, but not LB male offspring. This is consistent with a previous report showing that fear-induced increase in the firing rates of IL neurons is much weaker than that of PL neurons and that spontaneous neuronal firing measured by single-unit recording is sustainedly decreased in a subgroup of IL neurons during the recovery period after fear

conditioning in adult male rats (Fitzgerald *et al.*, 2015). These results are consistent with our observation of subtle LB- and fear-induced changes in the prefrontal glutamatergic transmission in pre-adolescent rats, where fear conditioning significantly increase glutamatergic transmission above baseline at the beginning of fear conditioning in the PL, but not IL mPFC of NB pre-adolescent males. Other reports have documented that after ELS exposure, cFos expressing cells are increased in the PL, but not IL mPFC during fear memory retrieval 24 hours after the fear conditioning in adolescent rats (PND45) (Junod *et al.*, 2019).

Effects of LB conditions on the maturation of parvalbumin interneurons in the mPFC

Interneurons are essential components of mPFC activity as they regulate long-range glutamatergic inputs to the mPFC originating from the BLA, vHIP, and other brain regions (Yang *et al.*, 2021). Specifically, parvalbumin (PV) interneurons constitute a large population in the mPFC and their protracted maturation from postnatal period to adolescence render them vulnerable to early adversities (Caballero *et al.*, 2014a). Formation of perineuronal nets (PNNs) around PV interneurons is associated with the maturation of these cells, coinciding with the termination of the critical periods of cortical plasticity (Guadagno *et al.*, 2021). In the present study, we wanted to determine whether LB conditions alter PV and PNN density in the mPFC of pre-adolescent rats (PND28-29) in a sex and region-specific manner and whether maturation of PV cells could in part explain the differences in prefrontal glutamatergic neurotransmission we observed during fear conditioning.

In the PL mPFC, NB male offspring displayed significantly lower density of PV interneurons than NB females, while there was a reduction in PNN expression in LB males compared to females. LB exposure specifically reduced the prelimbic co-expression of PV and

PNN in pre-adolescent male, but not female offspring. This is consistent with another report showing that PNN expression was transiently reduced by maternal separation in the PL mPFC of juvenile male and female offspring (PND20), although this difference did not persist into adolescence (PND40) and adulthood (Gildawie *et al.*, 2020). In the IL mPFC, LB exposure decreased the density of PV interneurons in both male and female offspring, but the co-expression of PV and PNN was reduced in males only, leaving the PNN expression unchanged. Considering that the expression of PV increases across development from juvenility to adolescence, our results indicate that LB conditions may delay or impair the expression of PV interneurons in the IL, but not PL mPFC of pre-adolescent rats. The region-dependent effects of LB on the prefrontal PV expression were not observed in the previously mentioned study using the maternal separation (MS) paradigm of early stress (Gildawie *et al.*, 2020).

When co-expression of PV/PNN is considered, an interesting pattern emerges. In both the PL and IL mPFC, LB specifically reduces co-expression of PV and PNN in males, but not female offspring. This suggests that LB exposure delays the maturation of PV interneurons in the PL and IL mPFC in a sex-dependent manner. We hypothesize that the sex-specific effects of ELS on the prefrontal maturation of PV interneurons are possibly mediated by ELS-induced alterations in oxidative and neuroinflammatory mediators, since fast-spiking PV interneurons require high energy supply and thus are very susceptible to oxidative stress and neuroinflammation (Ruden *et al.*, 2021). Indeed, elevated levels of pro-inflammatory cytokines (TNF-alpha and IL-6) were measured in the mPFC of MS-exposed males, but not females (González-Pardo *et al.*, 2020). The circulating expression of anti-inflammatory cytokine IL-10 was also found to be reduced by ELS in male offspring exclusively (Grassi-Oliveira *et al.*, 2016). Interestingly, (Gildawie *et al.*, 2021) using a two-hit adversity model consisting of postnatal MS and juvenile social isolation

demonstrated a similar pattern of reduced cell density of PNN surrounding PV interneurons in the mPFC, but with more pronounced effects in adult females compared to males. Differential alterations in the somatic development and sexual maturation that are induced by different forms of early adversity (Bath, 2020) as well as the different observation time might contribute to this discrepancy in the sex-dependent effects of ELS on the maturation of PV interneurons in the mPFC.

During fear acquisition, activation of PV interneurons inhibits principal neurons in the soma level and other types of interneurons, such as somatostatin (SST) interneurons also participate in modulating mPFC principal neurons. SST interneurons have a dual effect to disinhibit pyramidal neurons in the PL mPFC via their action on PV interneurons (Cummings & Clem, 2020) and to inhibit principal neurons at the axon terminal level (Anastasiades & Carter, 2021) Considering the role of PNNs in stabilizing neuronal inputs on PV interneurons (Carceller *et al.*, 2020), we propose that LB-induced delayed maturation of PV interneurons in the mPFC of pre-adolescent males might be associated with a reduction in SST- driven inhibitory inputs onto PV cells in the PL mPFC of these animals. Future experiments should examine whether a reduction in SST interneuron density in LB conditions would significantly affect PV activity in pre-adolescent rats as demonstrated following early disruption of prefrontal activity (Bitzenhofer *et al.*, 2021) The reduced inhibitory SST regulation on the prelimbic PV interneurons might induce inhibition of principal neurons in this region during fear conditioning in ELS-exposed pre-adolescent males. We are planning to conduct a triple fluorescence immunohistochemistry with cFos, PV, and SST on the brain sections collected from NB and LB offspring after fear conditioning to investigate this speculation.

F. Conclusions

In summary, our experiments demonstrate that the effects of LB conditions on the prefrontal glutamatergic transmission during fear conditioning are age-, sex- and region-dependent. LB exposure enhances fear-induced glutamate release in the PL mPFC of adult males, while the opposite trend is observed in pre-adolescent male, but not female offspring. We hypothesize that the effects of LB on mPFC glutamatergic neurotransmission are mediated by both alterations in the development of glutamatergic projections targeting the mPFC and in the maturation of local inhibitory circuits. Indeed, we found that LB exposure delays the maturation of prefrontal PV interneurons in a sex-dependent pattern, where the density of PV cells surrounded by PNN in the PL and IL mPFC is decreased in the LB-reared male, but not female pre-adolescent rats. These studies highlight important developmental processes leading to the modifications in adult functional and behavioral phenotypes induced by early life stress.

G. Figures

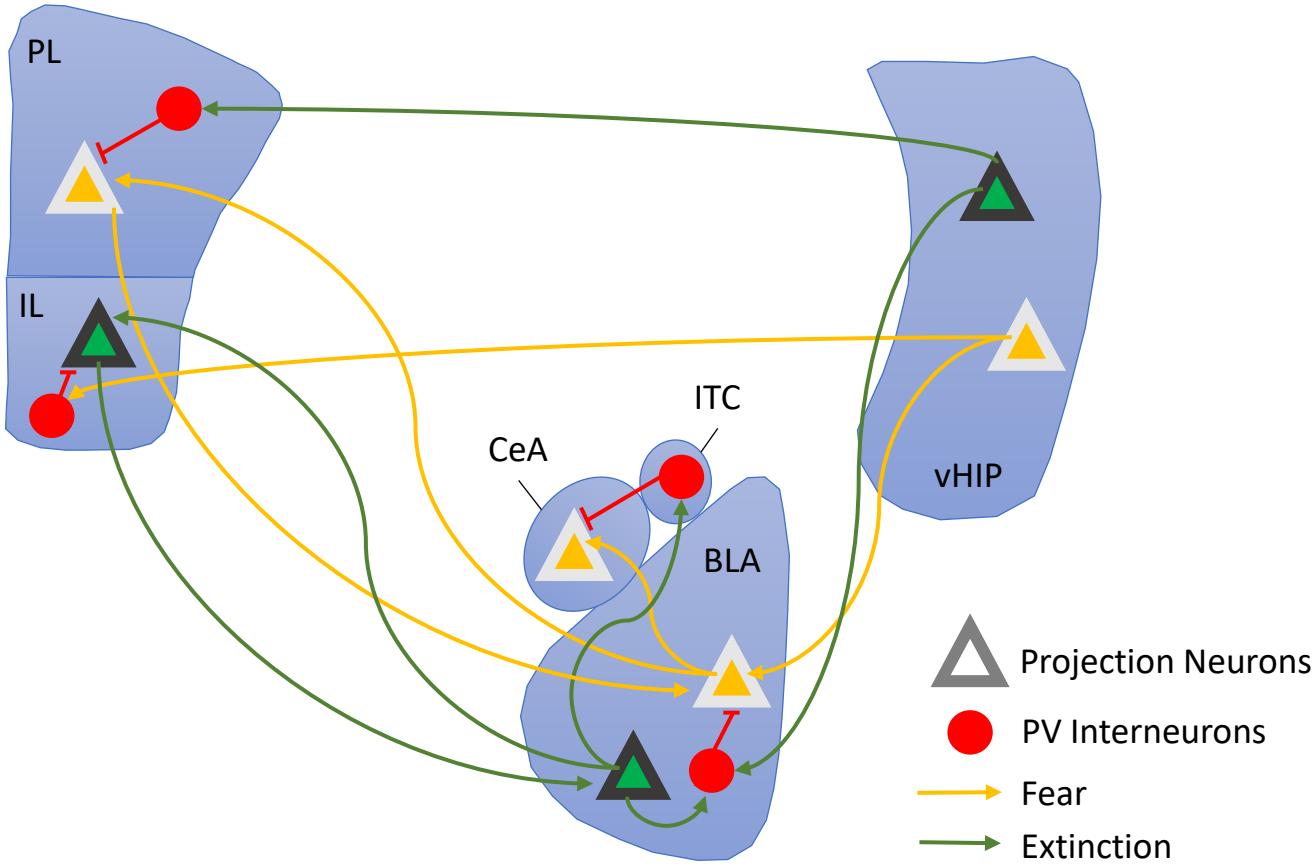

Figure 1:

Simplified schematic illustration of corticolimbic pathways for fear (yellow) and extinction (green). Fear expression and fear extinction are thought to be mediated by the prelimbic (PL) and infralimbic (IL) medial prefrontal cortex (mPFC). The PL-BLA projection promotes fear expression by connecting to pyramidal neurons in the central amygdala (CeA), whereas the IL-BLA projection promotes fear extinction by driving feedforward inhibition to the CeA via the intercalated cells (ITCs). Fear- and extinction-driven projection neurons in the basolateral amygdala (BLA) target preferentially to projection neurons in the PL and IL mPFC, respectively. The ventral hippocampal (vHIP) inputs to the mPFC, on the other hand, preferentially synapse onto inhibitory parvalbumin (PV) interneurons in the mPFC. The vHIP also indirectly regulates mPFC activity via its innervations in the BLA.

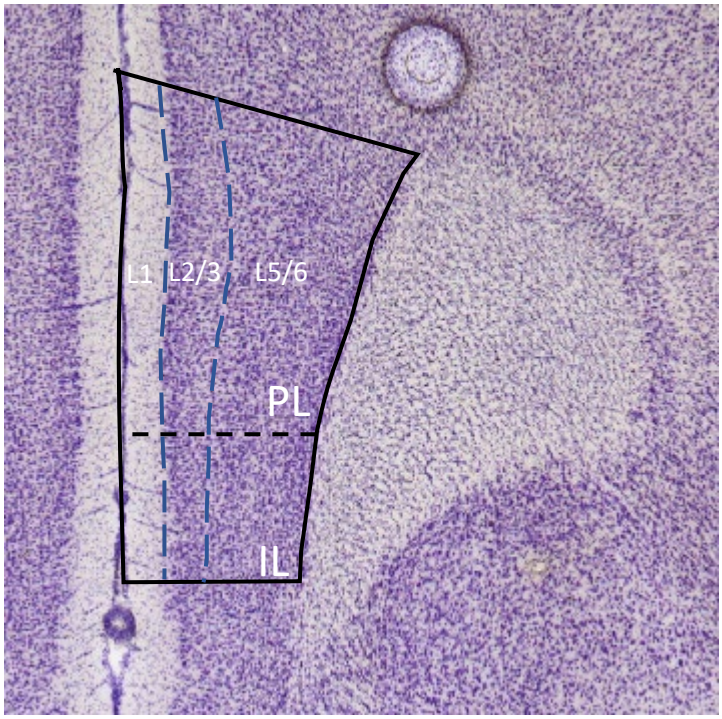

Bregma 3.0 mm

Figure 2:

Illustration of laminar organizations in the mPFC. The image of the coronal section of the mPFC stained with cresyl violet is adapted from the Paxinos atlas (Paxinos & Watson, 2005). The cortical layers (L) and the prelimbic (PL) and the infralimbic (IL) regions of the mPFC are outlined.

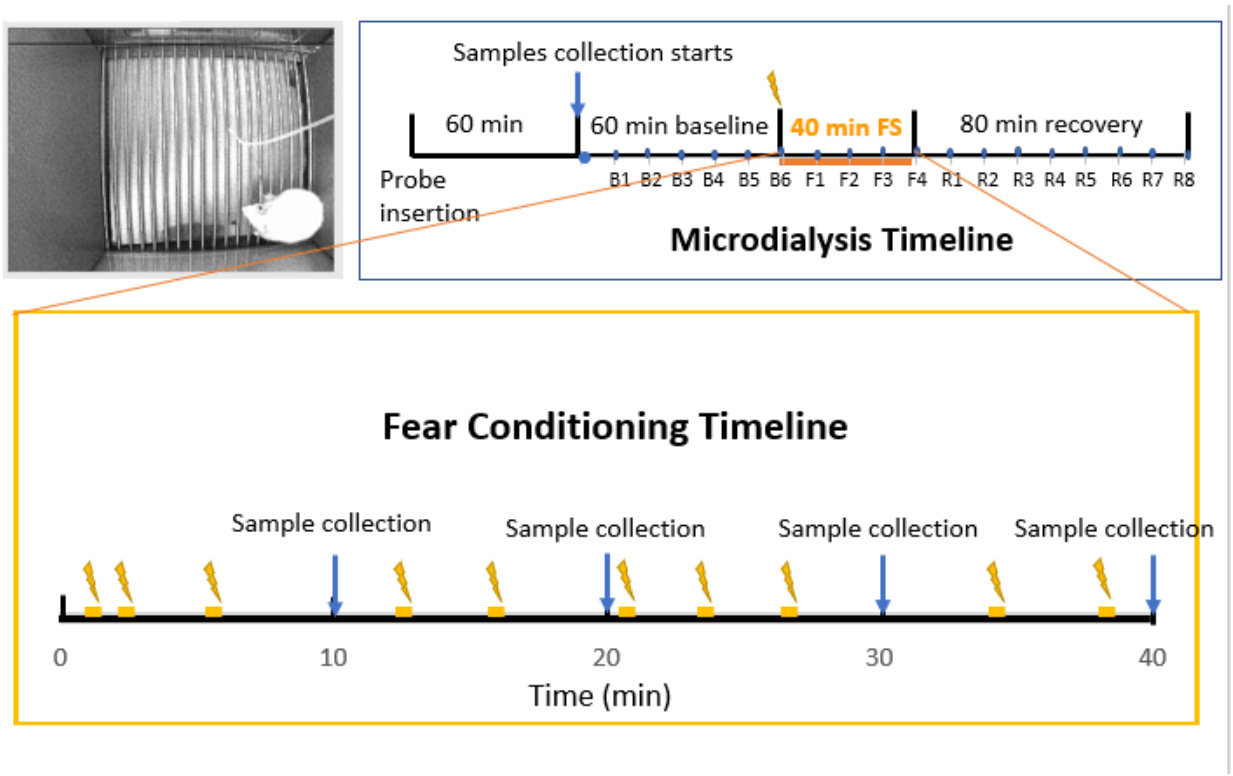

Figure 3:

Representative timelines of *in vivo* microdialysis. A microdialysis probe was inserted into the pre-implanted guide cannula on the day of the testing and perfused with aCSF at a constant flow rate of 1ul/min. After a one-hour wash period, microdialysates were collected every 10 minutes during baseline (60 minutes, sample B1-6), fear conditioning (40 minutes, sample F1-4), and recovery (80min, sample R1-8). A zoomed-in timeline of the 40 min fear conditioning session is displayed at the bottom. During fear conditioning, 10 tone-shock (co-terminating with the tone) pairings with an average of 4 min variable intertrial interval were delivered. Yellow lines and shock markers represent 30 seconds of tones and 0.5 seconds of foot shocks, respectively. The timepoints of sample collection are indicated by blue arrowheads.

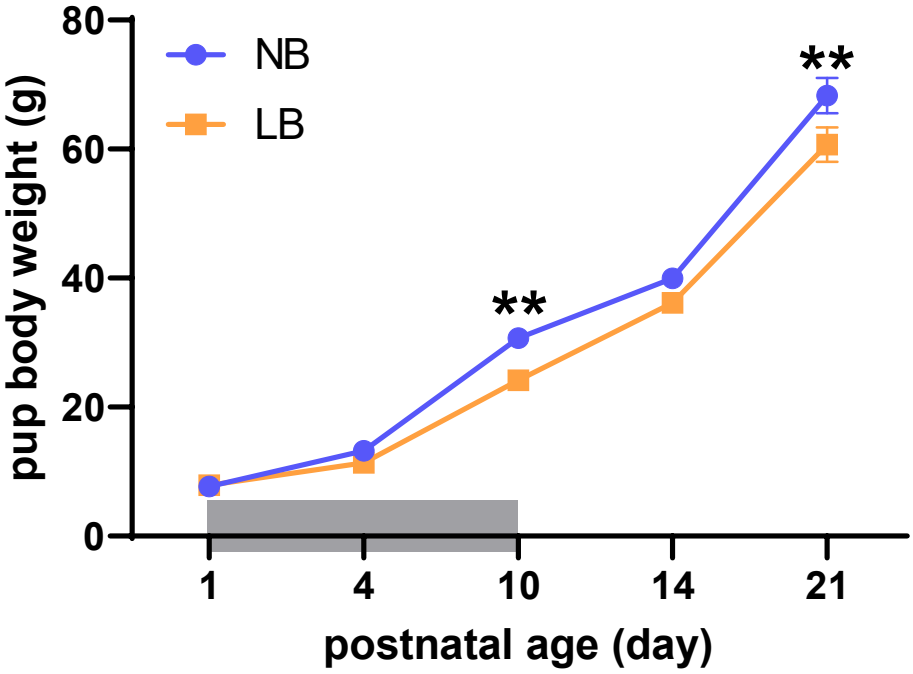

Figure 4:

Body weight gain of LB pups was lower than that of NB pups. There were 9-10 pups in each litter and body weight was measured on PND1, PND4, PND10, PND14, and PND21. Two-way ANOVA with bedding (NB vs. LB) and age (repeated) as factors showed a significant effect of bedding ($p<0.05$), age ($p<0.001$) and a significant bedding x age interaction ($p<0.05$). Grey bar represents the duration of bedding condition treatment. All values are represented as mean +/- SEM. n=8 litters per bedding group. **, $p<0.01$ Bonferroni post-hoc test for NB vs LB groups.

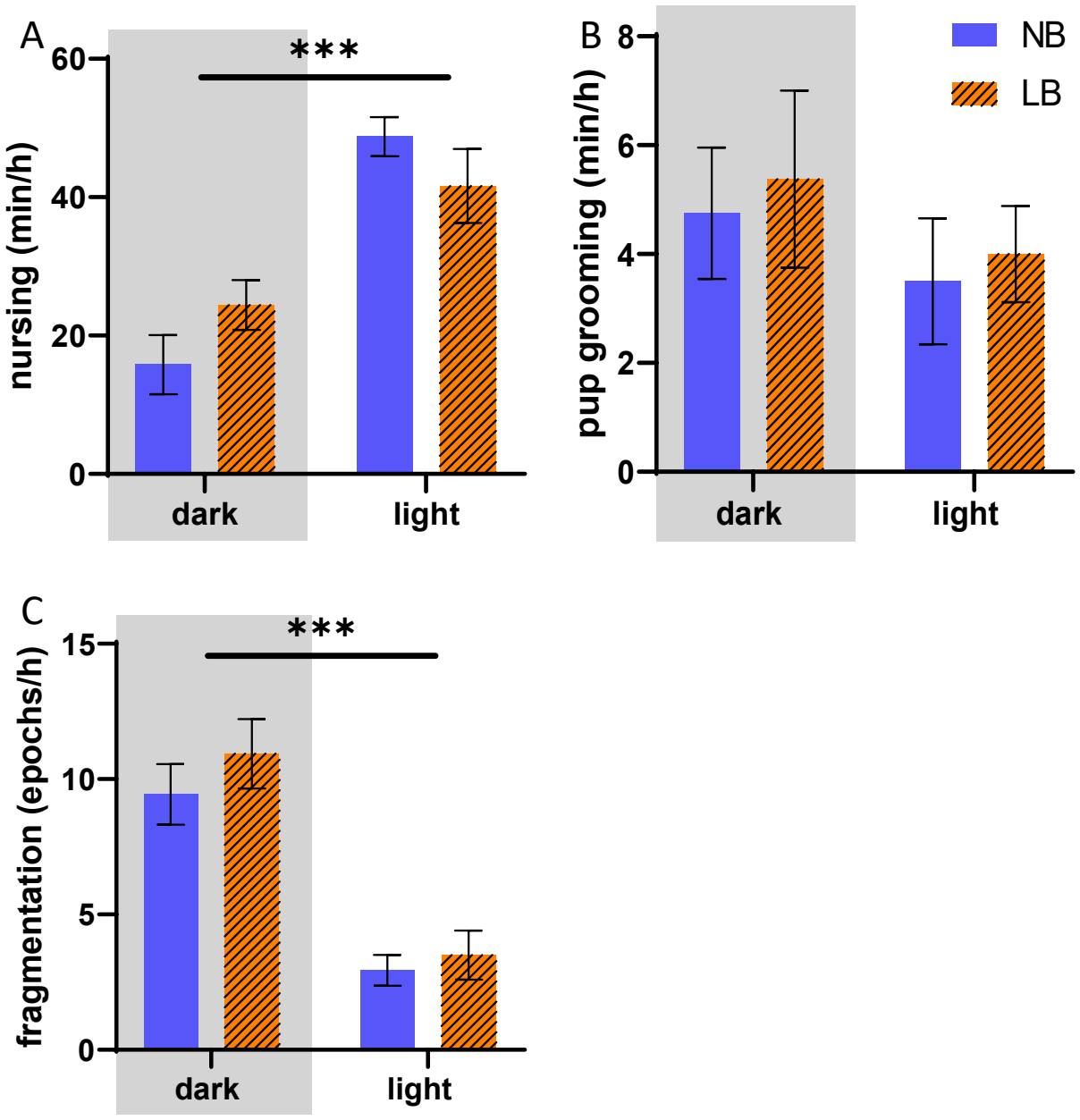

Figure 5:

Maternal behavior scores in NB condition and LB condition. (A) Total nursing behavior (both active and passive), (B) pup grooming behavior, (C) and fragmentation of maternal behavior were recorded between PND5-6 were compared between light phase and dark phase (shaded). Values represent the average of two observations per light period. Two-way ANOVA tests showed a significant main effect of light phase ($p<0.001$) for nursing and fragmentation. All values are represented as mean +/- SEM. n=8 mothers per bedding group. ***, $p<0.001$ dark vs. light phase

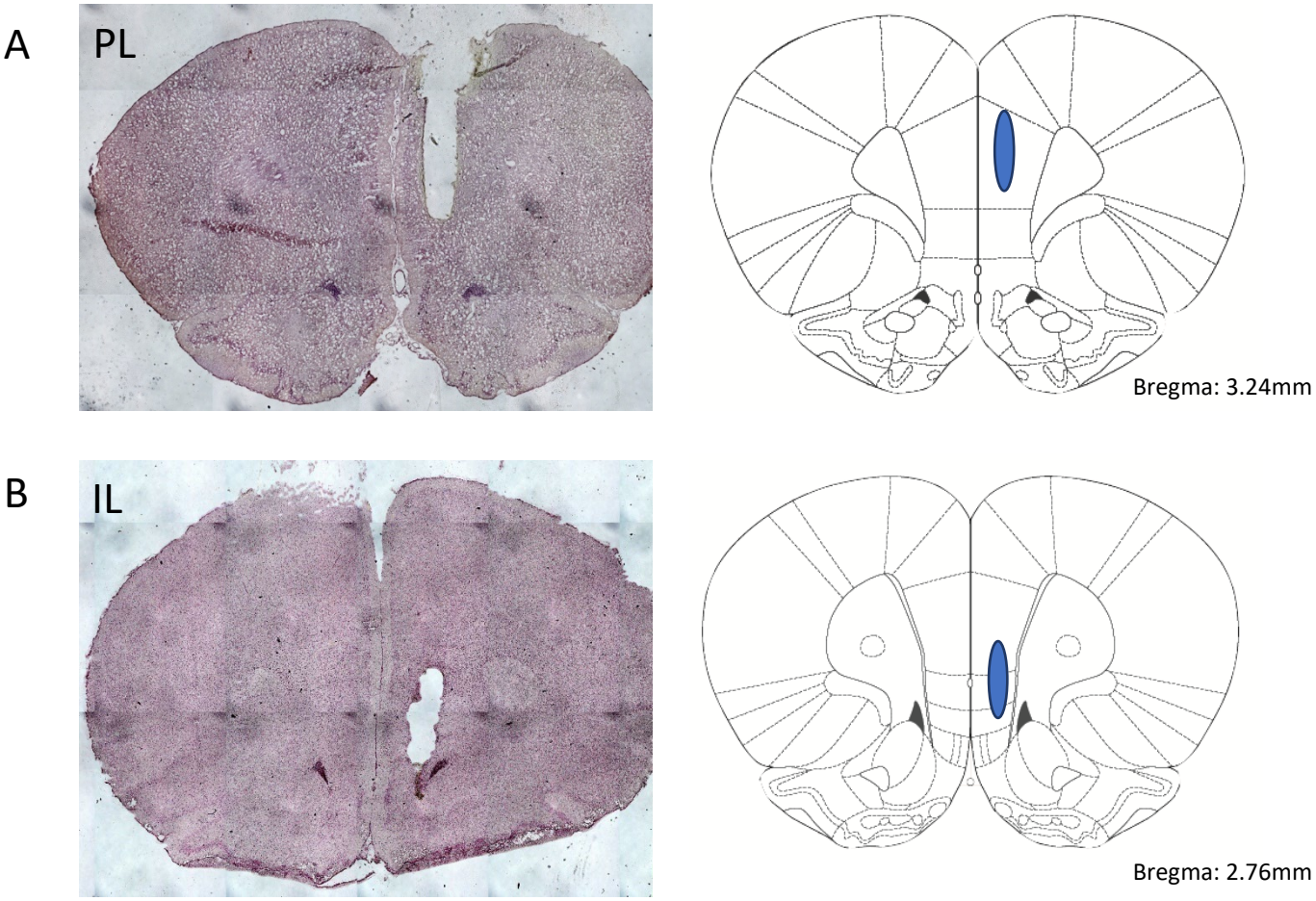

Figure 6:

Representatives of microdialysis probe placement in (A) PL and (B) IL mPFC in pre-adolescent rats. Left: Coronal brain sections of 20 um stained with cresyl violet. Images were taken in bright field at 4X (Olympus BX63). Right: Illustrations of the shape and distribution of the probe placements on the Paxinos atlas (Paxinos & Watson, 2005). Length of the blue bar corresponds to the 1.5 mm length of the active membrane of the microdialysis probe. Placements that were outside of these coordinates were excluded from our analyses (PL: pre-adolescent male, NB n=13, LB n=17; pre-adolescent female, NB n=10, LB n=13; adult male, NB n=12, LB n=13. IL: pre-adolescent male, NB n=10, LB n=6).

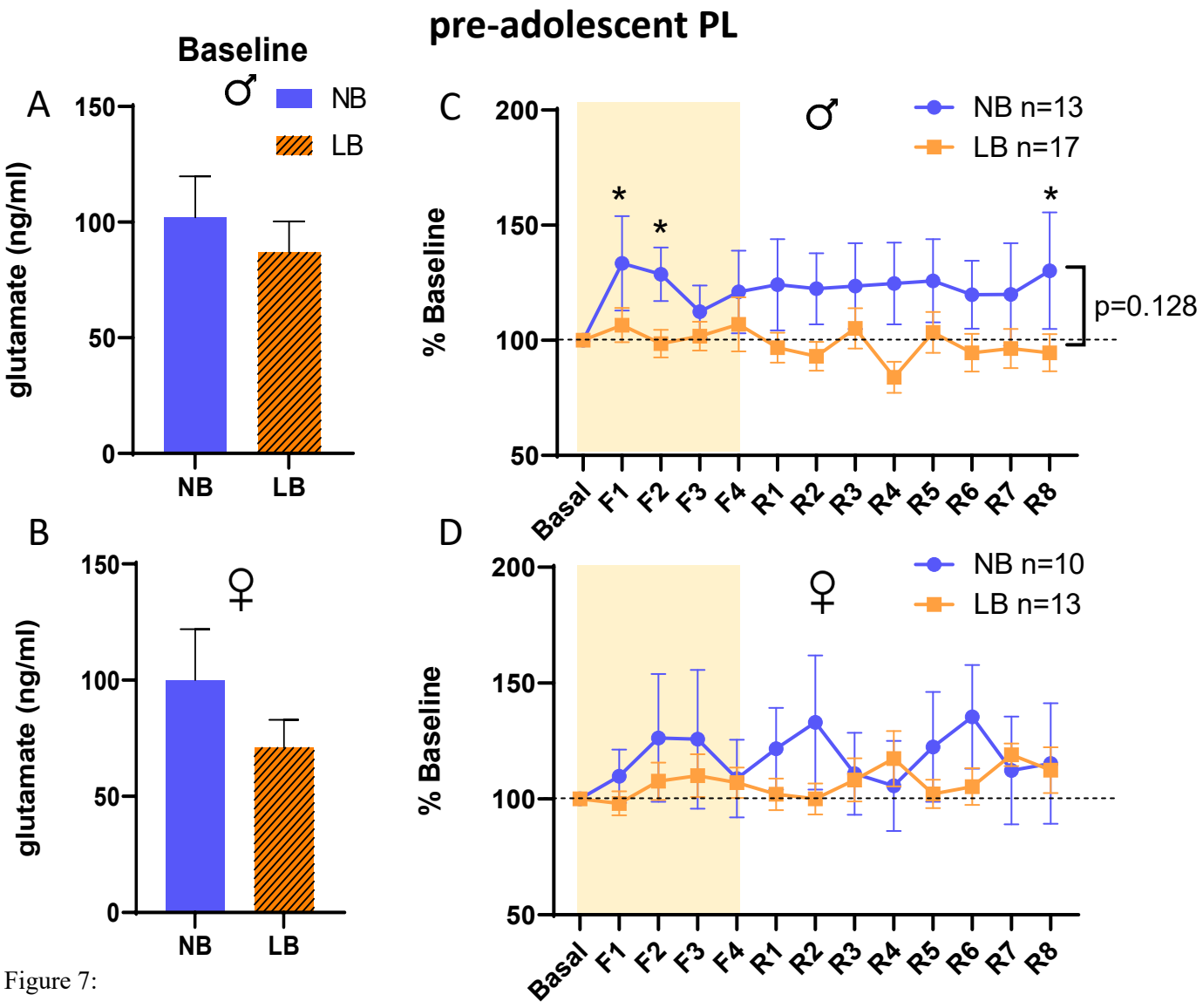

Figure 7:

Basal concentrations and fear-induced changes in the extracellular glutamate concentrations of dialysates collected from the right PL mPFC of NB and LB pre-adolescent male and female rats. Left: Pooled basal levels of glutamate concentrations in the six dialysate samples collected in the right PL mPFC of NB vs. LB pre-adolescent (A) males and (B) females before fear conditioning. There were no significant differences between NB and LB offspring in the basal levels of glutamate in the right PL mPFC in either pre-adolescent males or females. Right: Extracellular glutamate concentrations normalized as percentage of baseline in the right PL mPFC of NB vs. LB pre-adolescent (C) males and (D) females during (F1-F4) and after (R1-R8) fear conditioning. Shaded areas represent the 40 min duration of fear conditioning. LB exposure tended to suppress fear-induced glutamate response in the PL mPFC of pre-adolescent males ($p=0.128$), but not females. In males, significant increases in glutamate concentrations compared to baseline at F1, F2, and R8 were observed in NB offspring only ($p<0.05$). All values are represented as mean +/- SEM. n=10-17 per group. *, $p<0.05$ Dunnett's post-hoc test in NB group.

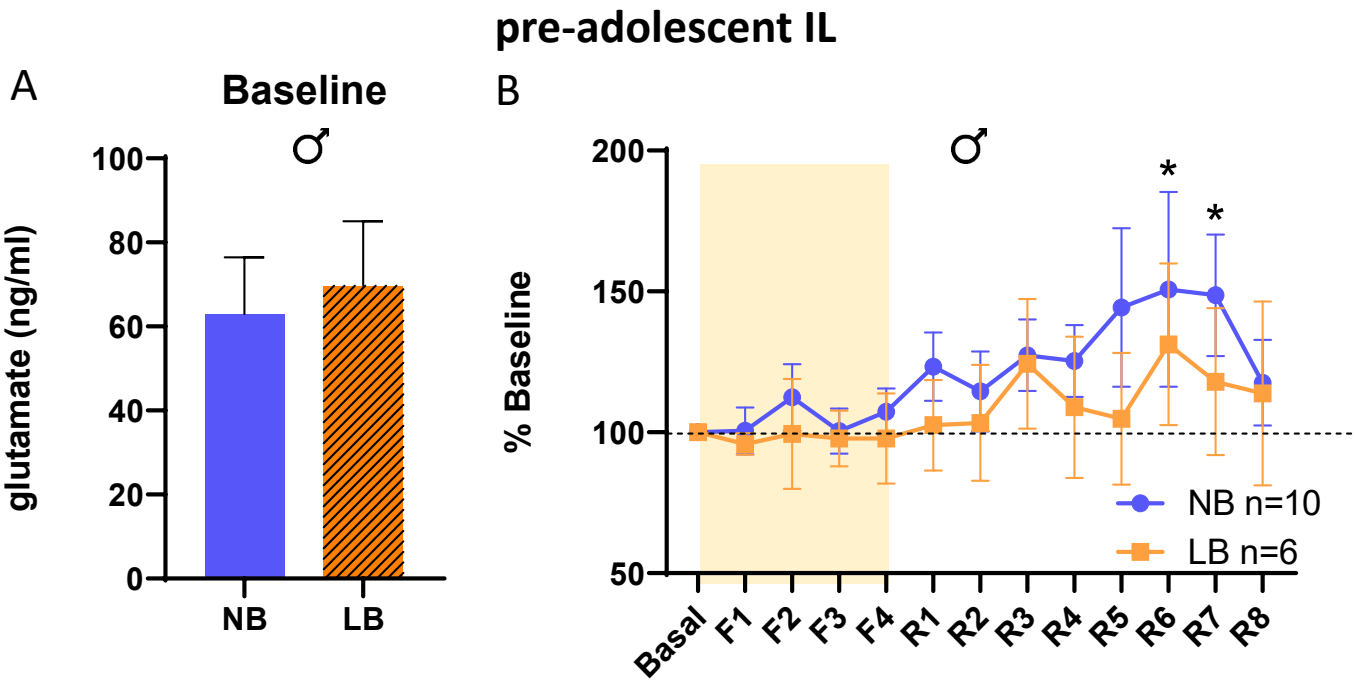

Figure 8:

Basal concentrations and fear-induced changes in the extracellular glutamate concentrations of dialysates collected from the right IL mPFC of NB and LB pre-adolescent males. (A) Pooled basal levels of glutamate concentrations in the six dialysate samples collected in the right IL mPFC of NB vs. LB pre-adolescent males before fear conditioning. No significant effect of bedding conditions found in the basal levels of glutamate in the right IL mPFC. (B) Extracellular glutamate concentrations normalized as percentage of baseline in the right IL mPFC of NB vs. LB pre-adolescent males during (F1-F4) and after (R1-R8) fear conditioning. Shaded areas represent the 40 min duration of fear conditioning. There was a significant effect of time ($p<0.05$), but no significant effect of bedding and no significant bedding x time interaction in the fear-induced glutamate response. All values are represented as mean +/- SEM. NB n=10, LB n=6. *, $p<0.05$ Dunnett's post-hoc test in NB group.

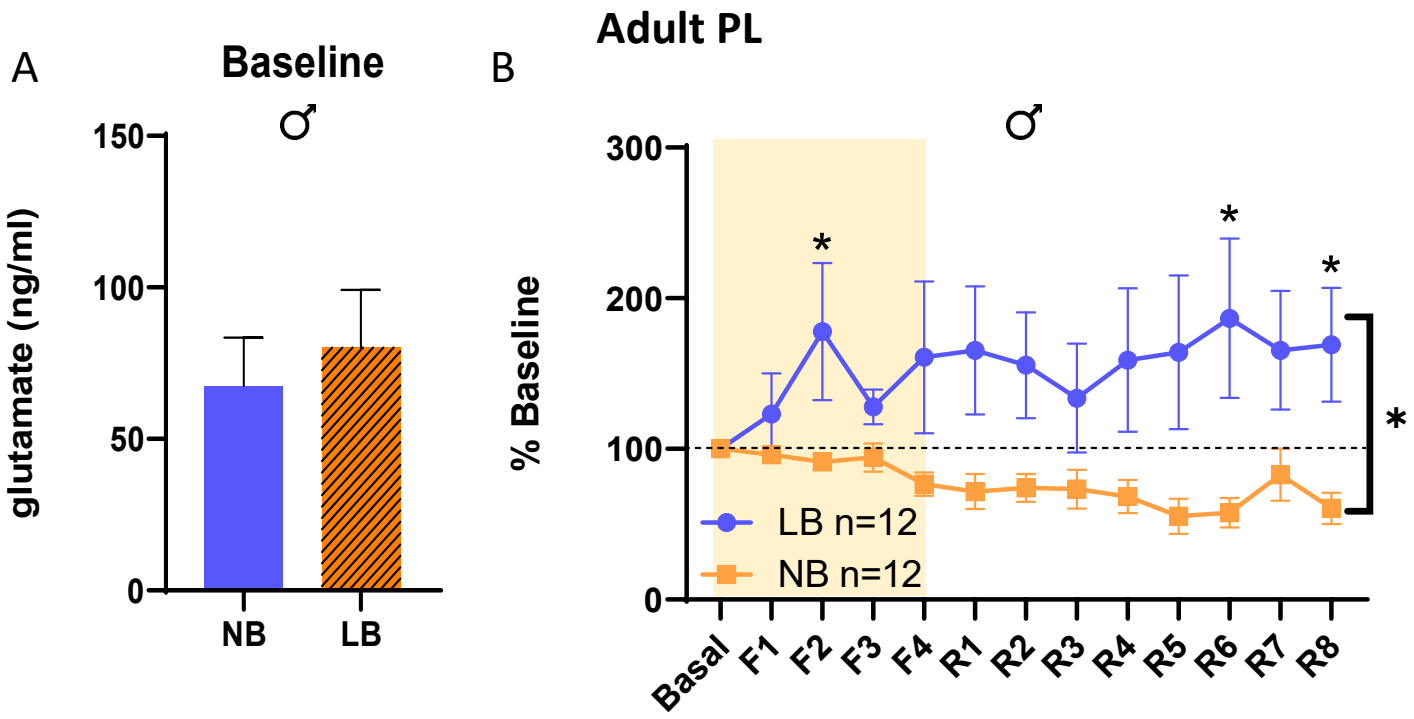

Figure 9:

Basal concentrations and fear-induced changes in the extracellular glutamate concentrations of dialysates collected from the right PL mPFC of NB and LB adult males. (A) Pooled basal levels of glutamate concentrations in the six dialysate samples collected in the right PL mPFC of NB vs. LB adult males before fear conditioning. There were no significant differences between NB and LB adult male offspring in the basal levels of glutamate in the right PL mPFC. (B) Extracellular glutamate concentrations normalized as percentage of baseline in the right IL mPFC of NB vs. LB adult males during (F1-F4) and after (R1-R8) fear conditioning. Shaded areas represent the 40 min duration of fear conditioning. The glutamate release in the right PL mPFC was significantly increased above baseline during (F2) and after (R6, R8) fear conditioning in the LB adult males ($p<0.05$), but not in NB controls (bedding effect $p<0.05$, bedding x time interaction $p=0.0940$). All values are represented as mean +/- SEM. n=12 in each bedding group. *, $p<0.05$.

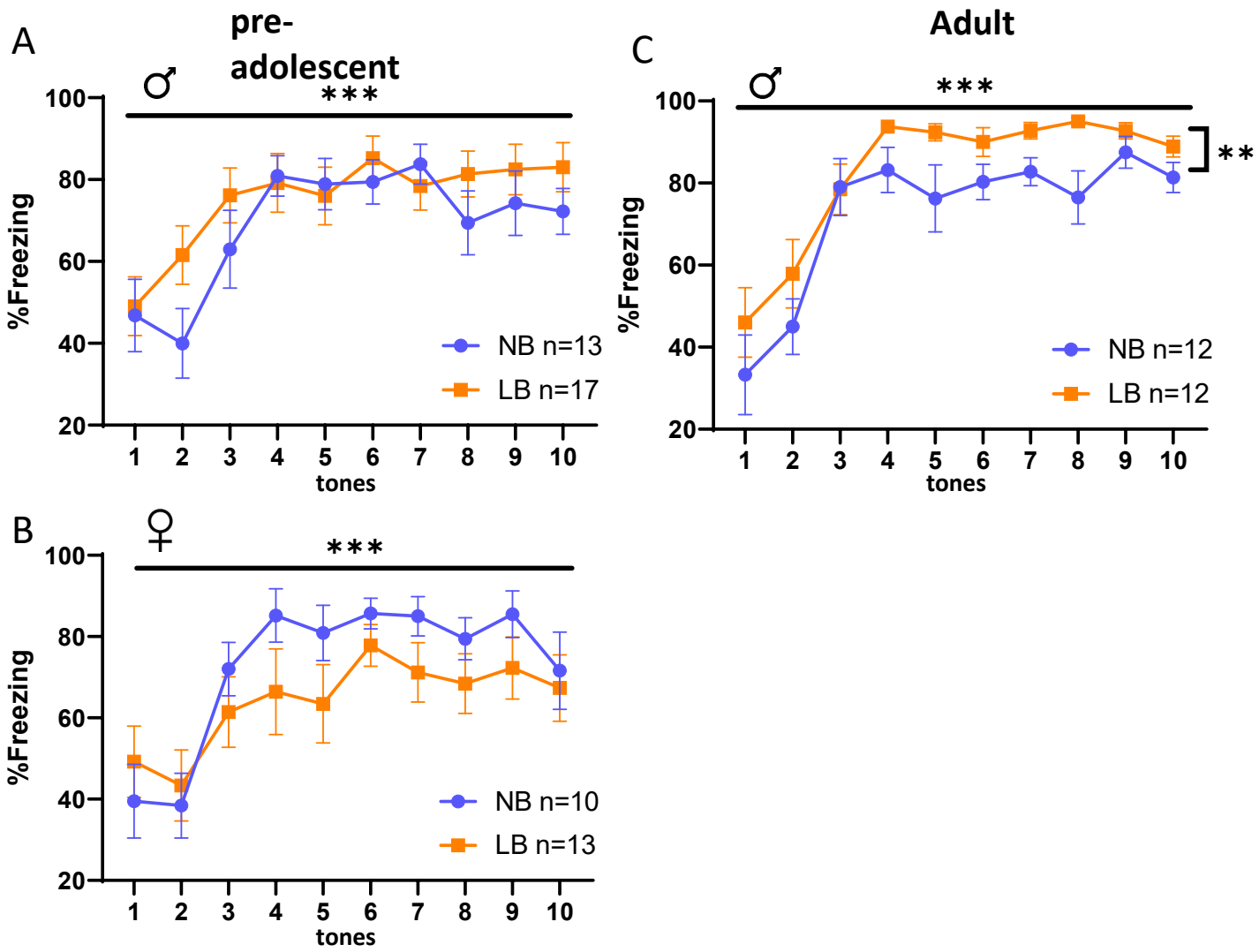

Figure 10:

Percentage of freezing time during exposure to ten tones paired with shocks in NB and LB offspring during PL mPFC microdialysis. (A) pre-adolescent males, (B) pre-adolescent females, (C) adult males. Although fear conditioning increased freezing behavior over ten tones in all groups of animals ($p<0.001$), there was a significant bedding effect only observed in adult males ($p<0.01$), where LB offspring displayed significantly more freezing behavior during tone-shock pairing compared to NB offspring. All values are represented as mean +/- SEM. n=10-17 in each group. **, $p<0.01$. ***, $p< 0.001$

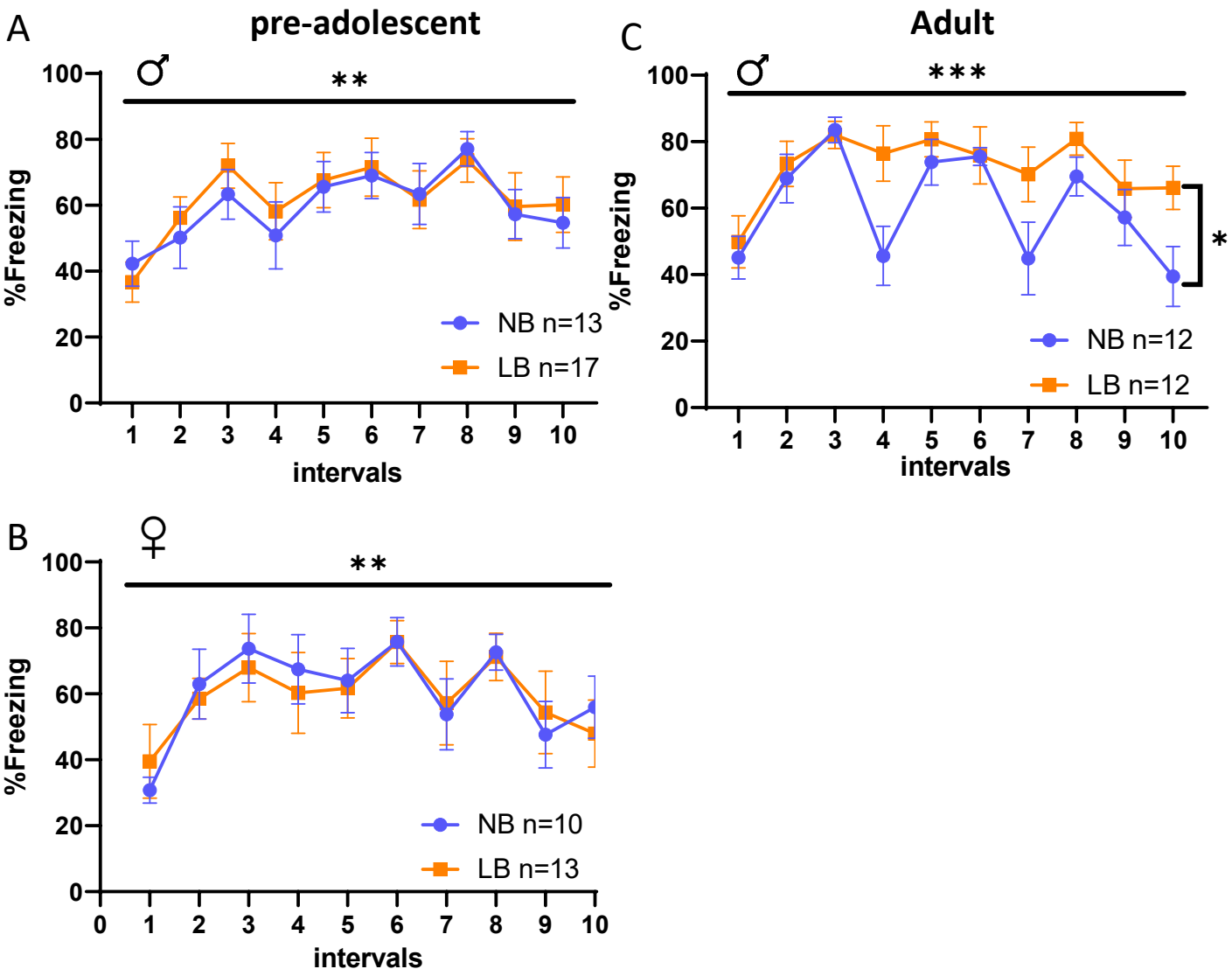

Figure 11:

Percentage of freezing time during intervals between conditioning tones in NB and LB offspring during PL mPFC microdialysis. (A) pre-adolescent males, (B) pre-adolescent females, (C) adult males. All groups of animals displayed increased freezing across intervals ($p<0.01$). In adult males only, there was a significant difference between bedding groups ($p<0.05$), where LB offspring exhibited significantly more freezing behavior than NB controls during intervals. All values are represented as mean +/- SEM. n=10-17 in each group. *, $p<0.05$. **, $p<0.01$. ***, $p< 0.001$

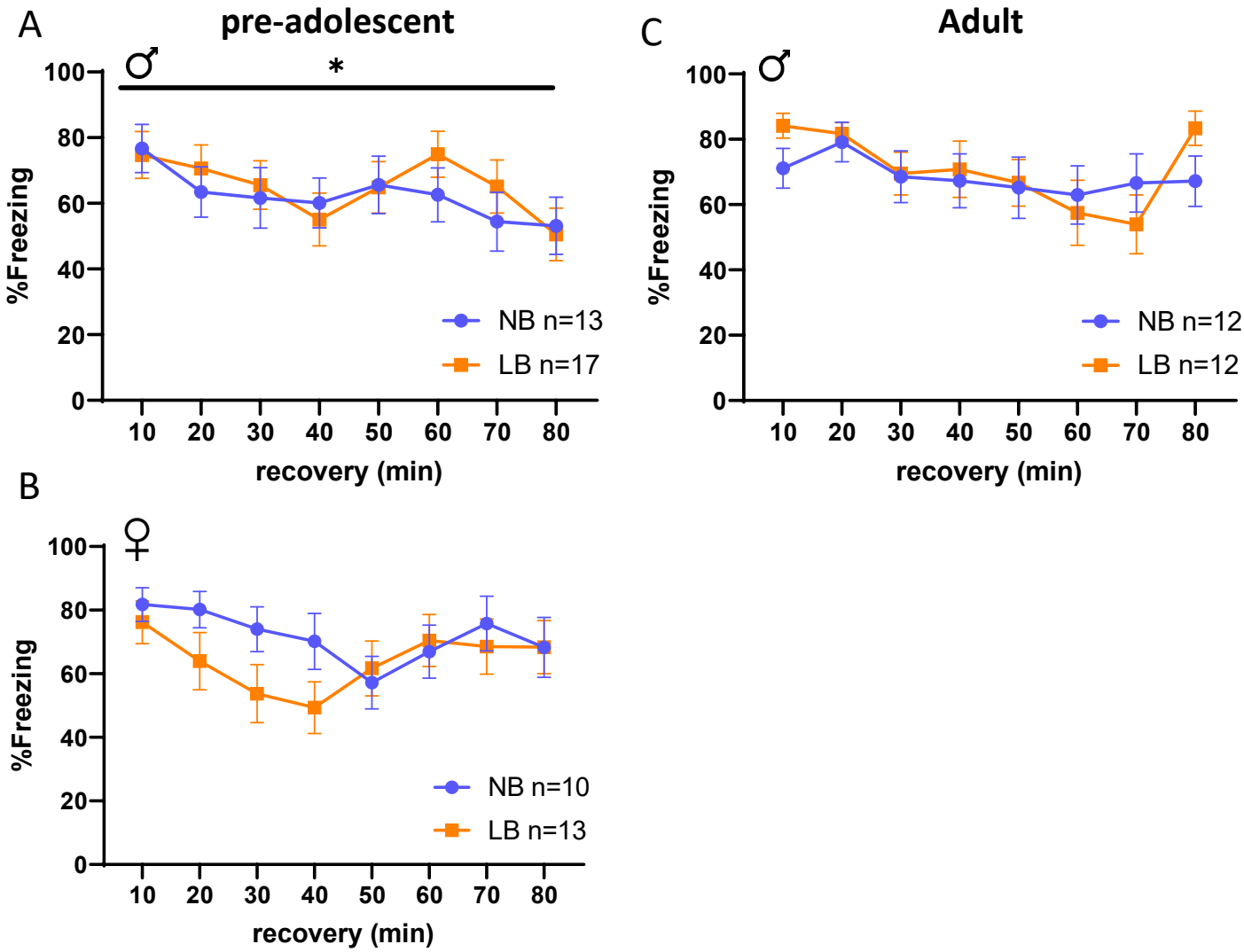

Figure 12:

Percentage of freezing time during the recovery from fear conditioning in NB and LB offspring during PL mPFC microdialysis. (A) pre-adolescent males, (B) pre-adolescent females, (C) adult males. Freezing behavior declined during recovery in pre-adolescent males only ($p<0.05$). There was no significant effect of bedding in any group of animals. All values are represented as mean +/- SEM. n=10-17 in each group. *, $p<0.05$.

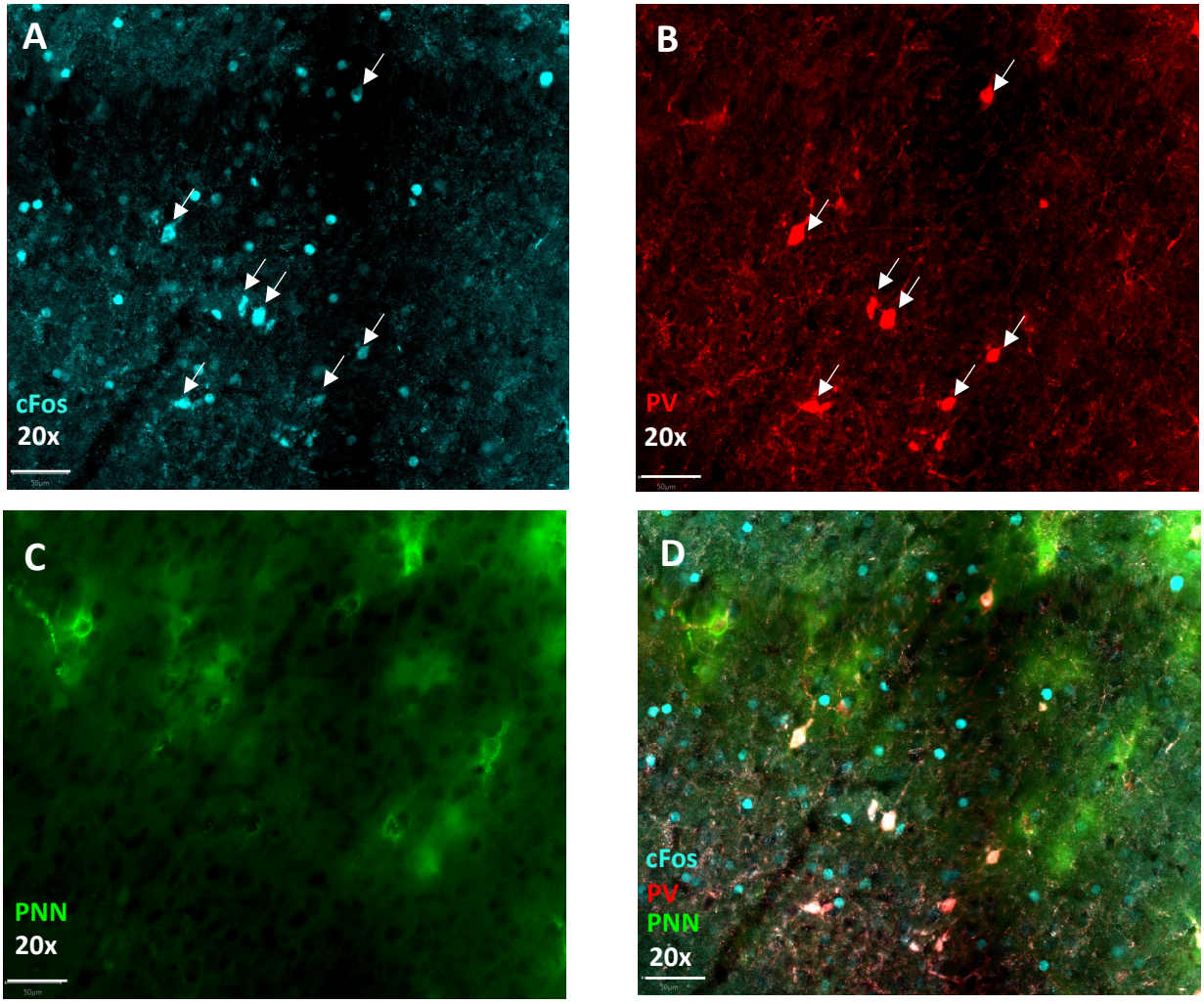

Figure 13:

Representative triple immunofluorescence staining images taken from the right mPFC in the PND28-29 rats showing (A) cFos positive (cyan), (B) PV positive (red), (C) PNN positive (green), and (D) merged expression of cFos, PV and PNN positive cells. White arrowheads indicate the overlap between the red fluorescence channel (PV) and the far-red fluorescence channel (cFos). Images were taken at 20x magnification and scale bars represent 50 um.

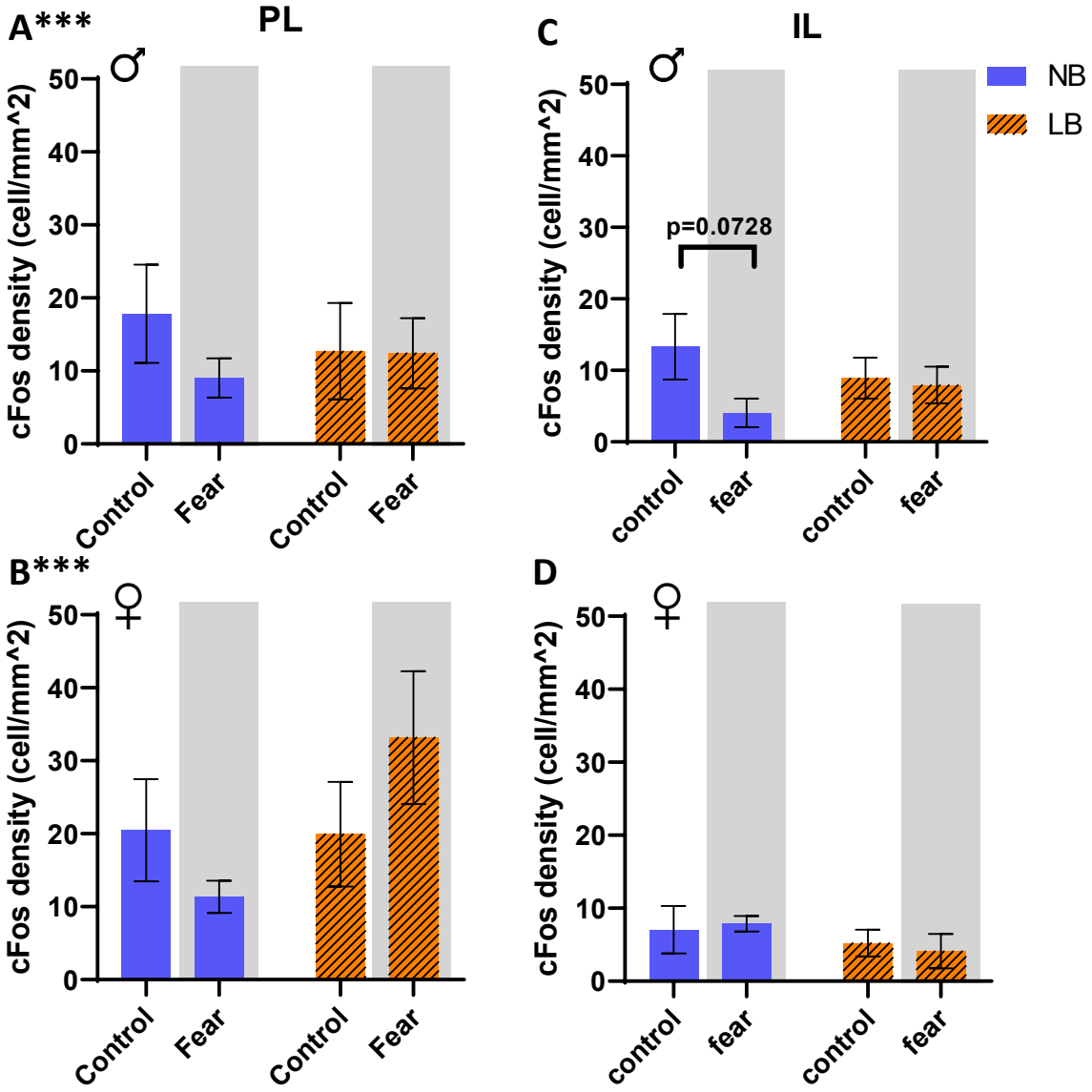

Figure 14:

Density of cFos positive cells after fear conditioning in the PL and IL mPFC of NB and LB male and female offspring on PND28-29. (A***) the PL mPFC of male offspring, (B***) the PL mPFC of female offspring, (C) the IL mPFC of male offspring, (D) the IL mPFC of female offspring. The brain tissues were collected from fear conditioning animals (shaded) or control animals 60 min after the onset of testing. Two-way ANOVA showed that the expression of cFos displayed no significant differences between fear treatments or bedding conditions in the PL and IL mPFC of male and female offspring. All values are represented as mean +/- SEM. n=5 per group.

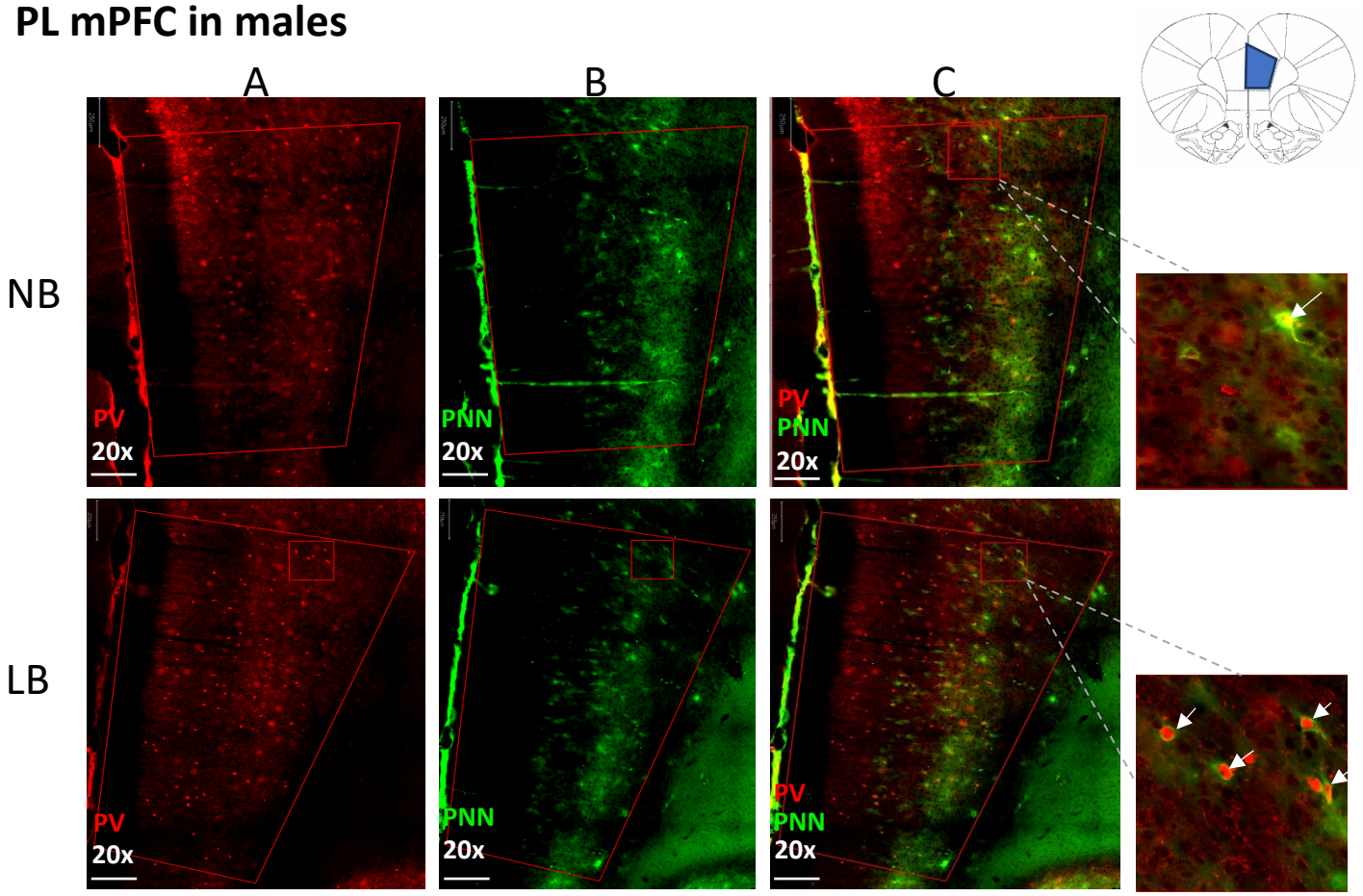

Figure 15:

Representative double immunofluorescence staining images taken from the right PL mPFC in the NB (upper panel) and LB (bottom panel) PND28-29 male offspring showing (A) PV positive (red), (B) PNN positive (green), and (C) the merged expression of PV and PNN positive cells. The PL region is outlined and the left side of the frame is aligned to midline. An enlargement of the red rectangle area is shown on the right and the cells co-expressing PV and PNN are indicated by white arrowheads. The images were taken at 20x magnification and scale bars represent 250 um.

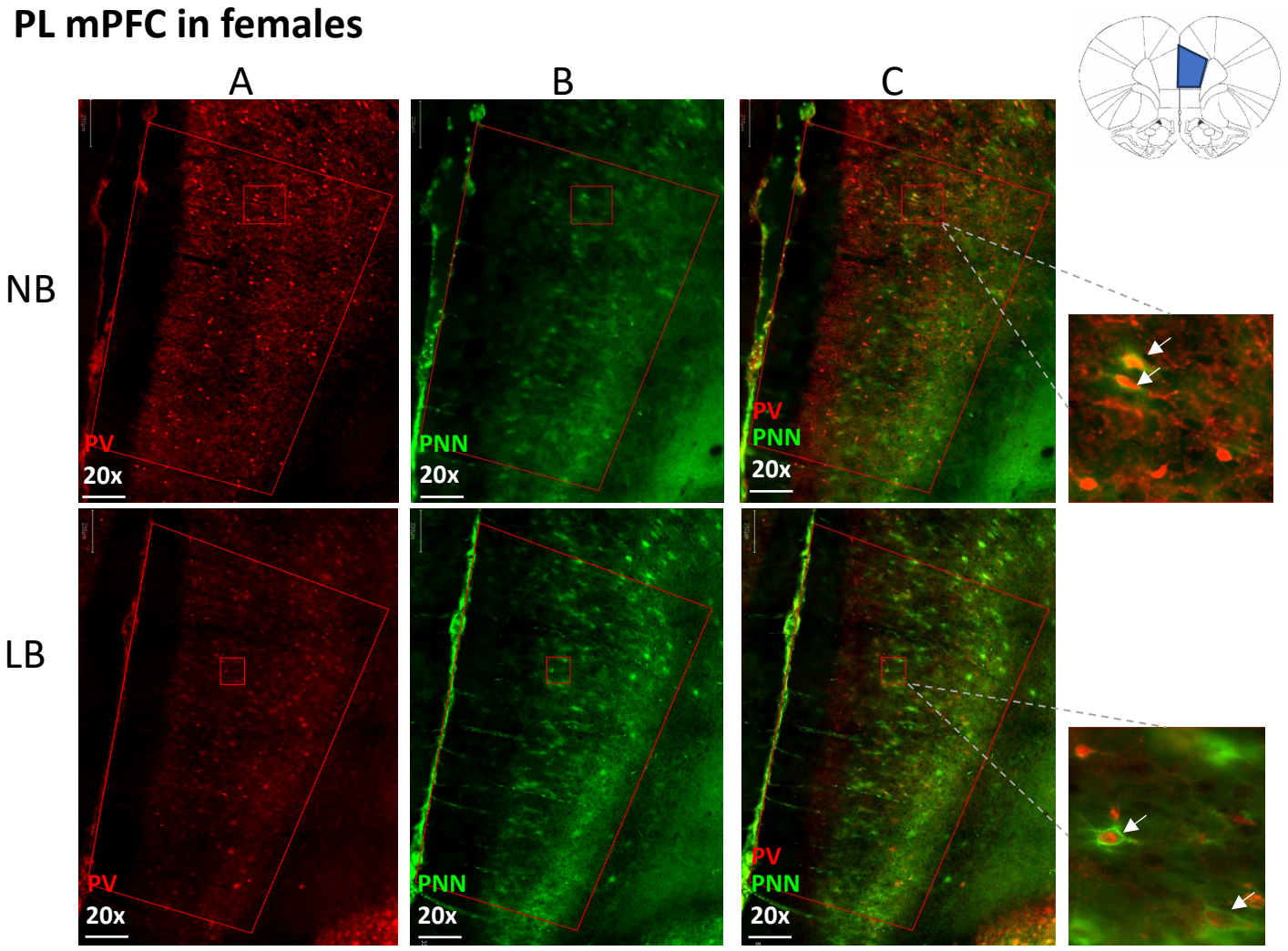

Figure 16:

Representative double immunofluorescence staining images taken from the right PL mPFC in the NB (upper panel) and LB (bottom panel) PND28-29 female offspring showing (A) PV positive (red), (B) PNN positive (green), and (C) the merged expression of PV and PNN positive cells. The PL region is outlined, and the left side of the frame is aligned to midline. An enlargement of the red rectangle area is shown on the right and the cells co-expressing PV and PNN are indicated by white arrowheads. The images were taken at 20x magnification and scale bars represent 250 um.

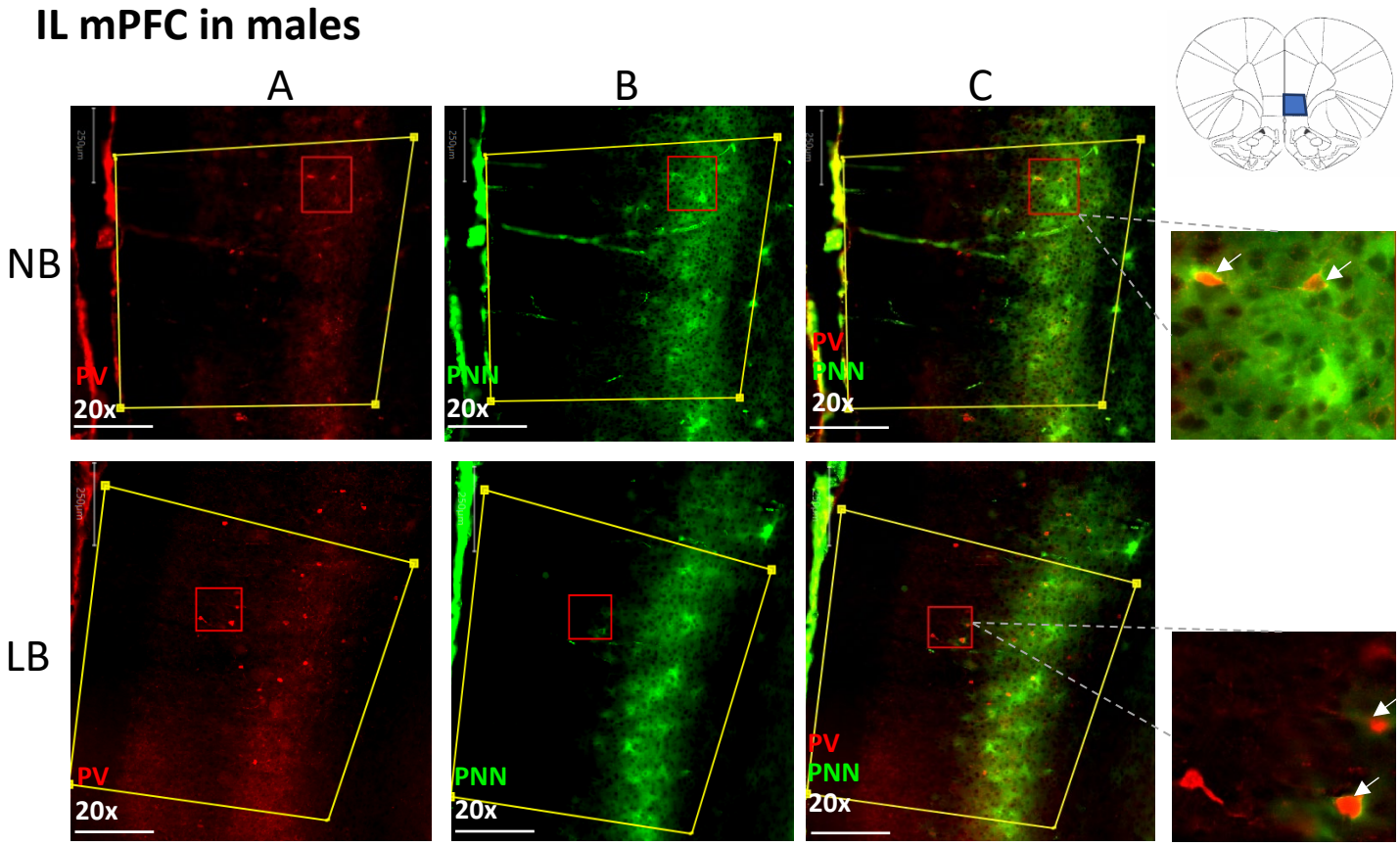

Figure 17:

Representative double immunofluorescence staining images taken from the right IL mPFC in the NB (upper panel) and LB (bottom panel) PND28-29 male offspring showing (A) PV positive (red), (B) PNN positive (green), and (C) the merged expression of PV and PNN positive cells. The IL region is outlined and the left side of the frame is aligned to midline. An enlargement of the red rectangle area is shown on the right and the cells co-expressing PV and PNN are indicated by white arrowheads. The images were taken at 20x magnification and scale bars represent 250 um.

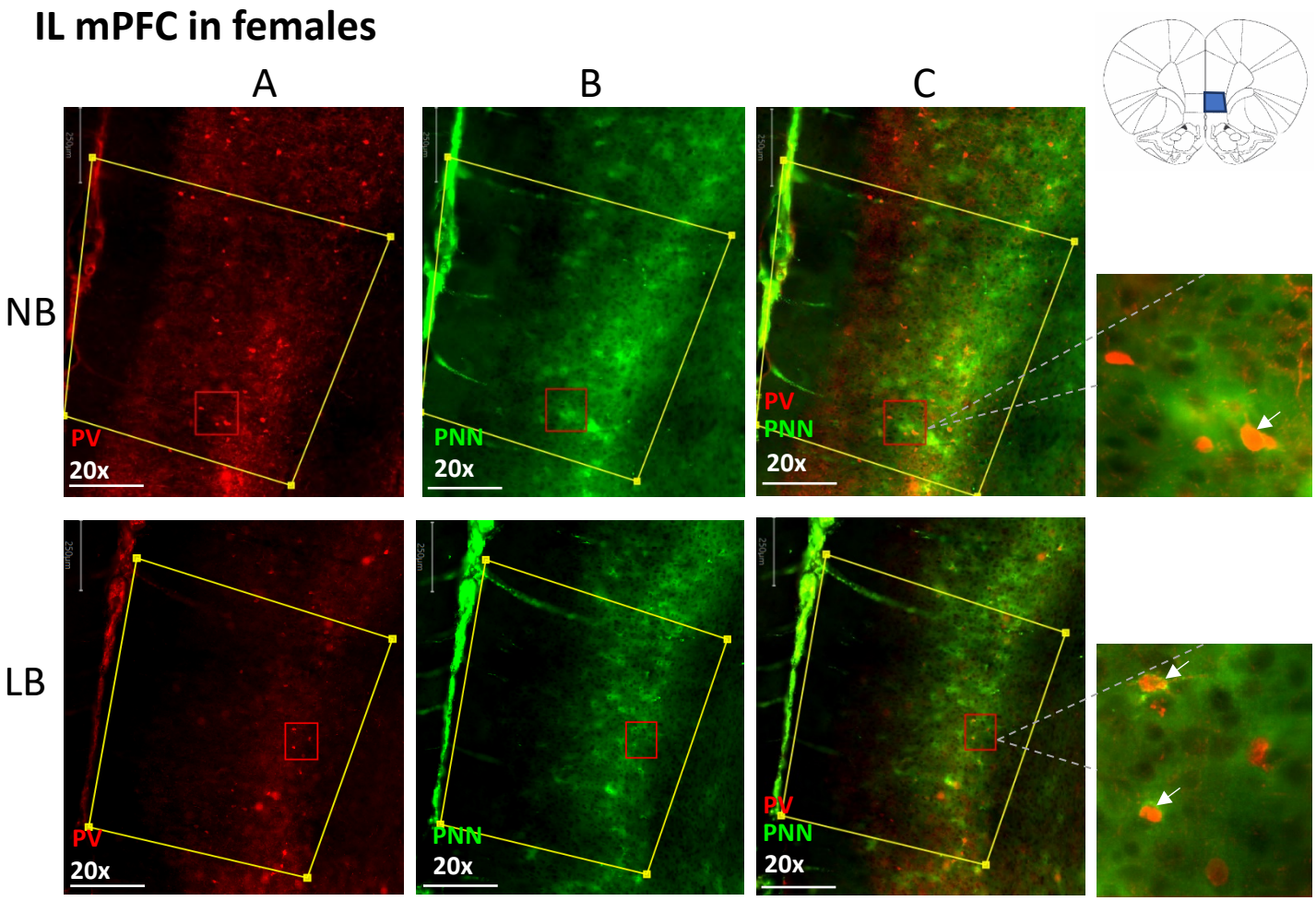

Figure 18:

Representative double immunofluorescence staining images taken from the right IL mPFC in the NB (upper panel) and LB (bottom panel) PND28-29 female offspring showing (A) PV positive (red), (B) PNN positive (green), and (C) the merged expression of PV and PNN positive cells. The IL region is outlined and the left side of the frame is aligned to midline. An enlargement of the red rectangle area is shown on the right and the cells co-expressing PV and PNN are indicated by white arrowheads. The images were taken at 20x magnification and scale bars represent 250 um.

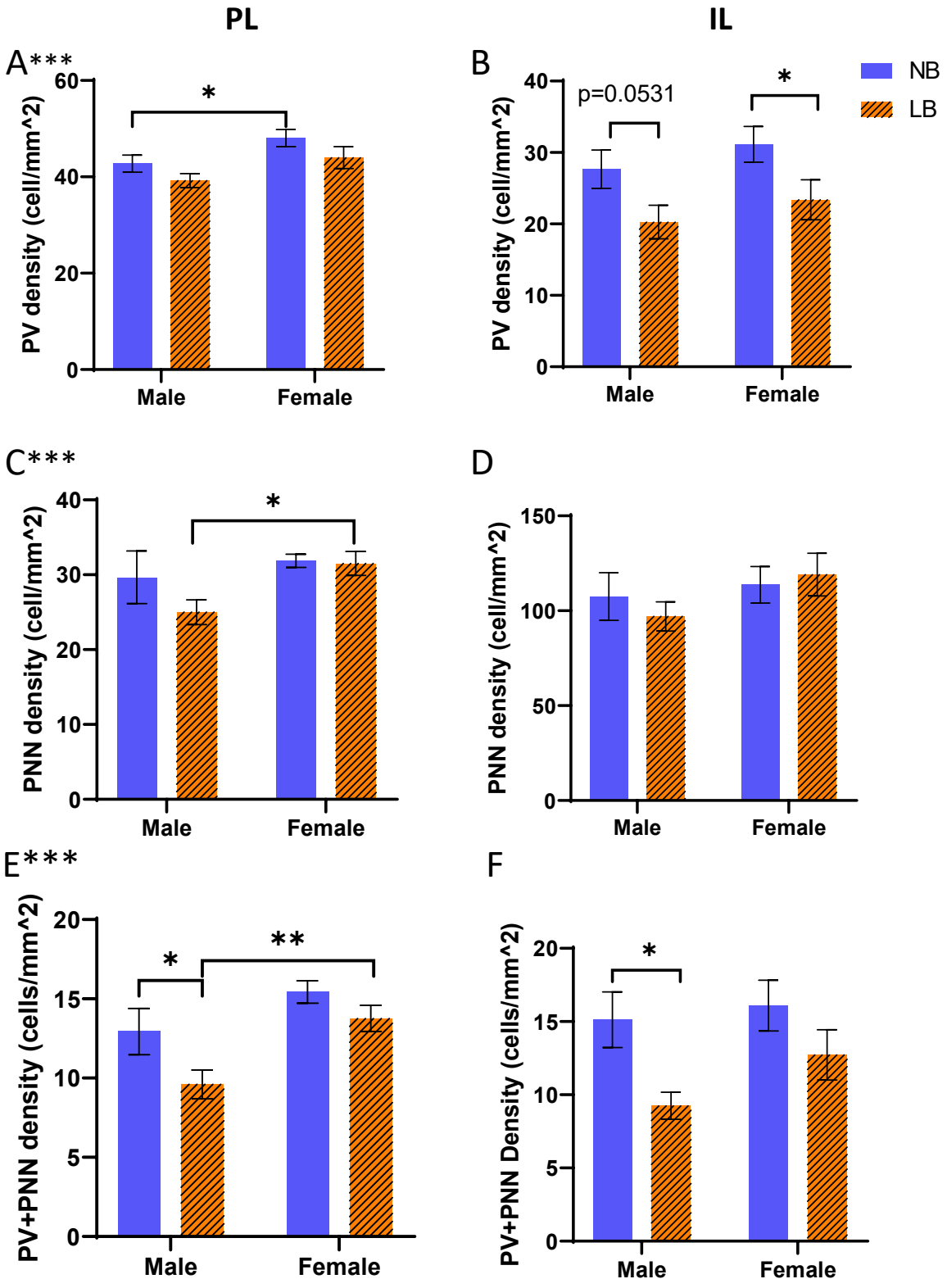
PL
IL
A***
B
C***
D
E***
F
NB
LB
p=0.0531
PV density (cell/mm^2)
PNN density (cell/mm^2)
PV+PNN density (cells/mm^2)
PV+PNN Density (cells/mm^2)
Male
Female
*
**

Figure 19:

Density of PV positive (A***, B), PNN positive (C***, D), and PV/PNN positive cells (E***, F) in the mPFC of NB and LB male and female offspring on PND28-29. In the PL mPFC, the differences between bedding conditions were significant in the density of PV positive ($p<0.05$) and PV/PNN positive cells ($p<0.05$), but not in the PNN cell density. We also observed significant effects of sex for PV ($p<0.01$) and for PV/PNN cell density ($p<0.01$), but not for PNN cell density in this region. In the IL mPFC, significant effects of bedding were observed for PV ($p<0.01$) and PV/PNN ($p<0.01$), but not for PNN cell density. There was no significant effect of sex for PV, PNN, and PV/PNN cell density in the IL mPFC of pre-adolescent offspring. No significant bedding x sex interaction was found in any two-way ANOVA test. All values are represented as mean +/- SEM. n=9-10 per group. *, $p<0.05$. **, $p<0.01$. ***, $p<0.001$. Bonferroni post-hoc test

H. References

An, B., Kim, J., Park, K., Lee, S., Song, S. & Choi, S. (2017) Amount of fear extinction changes its underlying mechanisms. *Elife*, **6**.

Anastasiades, P.G. & Carter, A.G. (2021) Circuit organization of the rodent medial prefrontal cortex. *Trends Neurosci*, **44**, 550-563.

Arp, J.M., Ter Horst, J.P., Loi, M., den Blaauwen, J., Bangert, E., Fernández, G., Joëls, M., Oitzl, M.S. & Krugers, H.J. (2016) Blocking glucocorticoid receptors at adolescent age prevents enhanced freezing between repeated cue-exposures after conditioned fear in adult mice raised under chronic early life stress. *Neurobiol Learn Mem*, **133**, 30-38.

Arruda-Carvalho, M., Wu, W.C., Cummings, K.A. & Clem, R.L. (2017) Optogenetic Examination of Prefrontal-Amygdala Synaptic Development. *J Neurosci*, **37**, 2976-2985.

Baker, K.D., Gray, A.R. & Richardson, R. (2017) The development of perineuronal nets around parvalbumin gabaergic neurons in the medial prefrontal cortex and basolateral amygdala of rats. *Behav Neurosci*, **131**, 289-303.

Barnet, R.C. & Hunt, P.S. (2006) The expression of fear-potentiated startle during development: integration of learning and response systems. *Behav Neurosci*, **120**, 861-872.

Bath, K.G. (2020) Synthesizing Views to Understand Sex Differences in Response to Early Life Adversity. *Trends Neurosci*, **43**, 300-310.

Baudin, A., Blot, K., Verney, C., Estevez, L., Santamaria, J., Gressens, P., Giros, B., Otani, S., Daugé, V. & Naudon, L. (2012) Maternal deprivation induces deficits in temporal memory and cognitive flexibility and exaggerates synaptic plasticity in the rat medial prefrontal cortex. *Neurobiol Learn Mem*, **98**, 207-214.

Bender, R.A., Zhou, L., Vierk, R., Brandt, N., Keller, A., Gee, C.E., Schäfer, M.K. & Rune, G.M. (2017) Sex-Dependent Regulation of Aromatase-Mediated Synaptic Plasticity in the Basolateral Amygdala. *J Neurosci*, **37**, 1532-1545.

Bitzenhofer, S.H., Pöpplau, J.A., Chini, M., Marquardt, A. & Hanganu-Opatz, I.L. (2021) A transient developmental increase in prefrontal activity alters network maturation and causes cognitive dysfunction in adult mice. *Neuron*, **109**, 1350-1364.e1356.

Bitzenhofer, S.H., Pöpplau, J.A. & Hanganu-Opatz, I. (2020) Gamma activity accelerates during prefrontal development. *Elife*, **9**.

Bolton, J.L., Molet, J., Ivy, A. & Baram, T.Z. (2017) New insights into early-life stress and behavioral outcomes. *Curr Opin Behav Sci*, **14**, 133-139.

Bolton, J.L., Molet, J., Regev, L., Chen, Y., Rismanchi, N., Haddad, E., Yang, D.Z., Obenaus, A. & Baram, T.Z. (2018) Anhedonia Following Early-Life Adversity Involves Aberrant Interaction of Reward and Anxiety Circuits and Is Reversed by Partial Silencing of Amygdala Corticotropin-Releasing Hormone Gene. *Biol Psychiatry*, **83**, 137-147.

Bouwmeester, H., Smits, K. & Van Ree, J.M. (2002) Neonatal development of projections to the basolateral amygdala from prefrontal and thalamic structures in rat. *J Comp Neurol*, **450**, 241-255.

Burgos-Robles, A., Kimchi, E.Y., Izadmehr, E.M., Porzenheim, M.J., Ramos-Guasp, W.A., Nieh, E.H., Felix-Ortiz, A.C., Namburi, P., Leppla, C.A., Presbrey, K.N., Anandalingam, K.K., Pagan-Rivera, P.A., Anahtar, M., Beyeler, A. & Tye, K.M. (2017) Amygdala inputs to prefrontal cortex guide behavior amid conflicting cues of reward and punishment. *Nat Neurosci*, **20**, 824-835.

Burgos-Robles, A., Vidal-Gonzalez, I. & Quirk, G.J. (2009) Sustained conditioned responses in prelimbic prefrontal neurons are correlated with fear expression and extinction failure. *J Neurosci*, **29**, 8474-8482.

Caballero, A., Flores-Barrera, E., Cass, D.K. & Tseng, K.Y. (2014a) Differential regulation of parvalbumin and calretinin interneurons in the prefrontal cortex during adolescence. *Brain Struct Funct*, **219**, 395-406.

Caballero, A., Flores-Barrera, E., Thomases, D.R. & Tseng, K.Y. (2020) Downregulation of parvalbumin expression in the prefrontal cortex during adolescence causes enduring prefrontal disinhibition in adulthood. *Neuropsychopharmacology*, **45**, 1527-1535.

Caballero, A., Thomases, D.R., Flores-Barrera, E., Cass, D.K. & Tseng, K.Y. (2014b) Emergence of GABAergic-dependent regulation of input-specific plasticity in the adult rat prefrontal cortex during adolescence. *Psychopharmacology (Berl)*, **231**, 1789-1796.

Caballero, A. & Tseng, K.Y. (2016) GABAergic Function as a Limiting Factor for Prefrontal Maturation during Adolescence. *Trends Neurosci*, **39**, 441-448.

Cabungcal, J.H., Steullet, P., Morishita, H., Kraftsik, R., Cuenod, M., Hensch, T.K. & Do, K.Q. (2013) Perineuronal nets protect fast-spiking interneurons against oxidative stress. *Proc*

Natl Acad Sci U S A, **110**, 9130-9135.

Caillard, O., Moreno, H., Schwaller, B., Llano, I., Celio, M.R. & Marty, A. (2000) Role of the calcium-binding protein parvalbumin in short-term synaptic plasticity. *Proc Natl Acad Sci U S A*, **97**, 13372-13377.

Callaghan, B.L. & Tottenham, N. (2016) The Stress Acceleration Hypothesis: Effects of early-life adversity on emotion circuits and behavior. *Curr Opin Behav Sci*, **7**, 76-81.

Carceller, H., Guirado, R., Ripolles-Campos, E., Teruel-Marti, V. & Nacher, J. (2020) Perineuronal Nets Regulate the Inhibitory Perisomatic Input onto Parvalbumin Interneurons and γ Activity in the Prefrontal Cortex. *J Neurosci*, **40**, 5008-5018.

Celio, M.R., Spreafico, R., De Biasi, S. & Vitellaro-Zuccarello, L. (1998) Perineuronal nets: past and present. *Trends Neurosci*, **21**, 510-515.

Cheriyan, J., Kaushik, M.K., Ferreira, A.N. & Sheets, P.L. (2016) Specific Targeting of the Basolateral Amygdala to Projectionally Defined Pyramidal Neurons in Prelimbic and Infralimbic Cortex. *eNeuro*, **3**.

Chini, M. & Hanganu-Opatz, I.L. (2021) Prefrontal Cortex Development in Health and Disease: Lessons from Rodents and Humans. *Trends Neurosci*, **44**, 227-240.

Chocyk, A., Bobula, B., Dudys, D., Przyborowska, A., Majcher-Maślanka, I., Hess, G. & Wędzony, K. (2013) Early-life stress affects the structural and functional plasticity of the medial prefrontal cortex in adolescent rats. *Eur J Neurosci*, **38**, 2089-2107.

Chocyk, A., Przyborowska, A., Makuch, W., Majcher-Maślanka, I., Dudys, D. & Wędzony, K. (2014) The effects of early-life adversity on fear memories in adolescent rats and their persistence into adulthood. *Behav Brain Res*, **264**, 161-172.

Cochran WC, Cox GM. (1957). Experimental designs. 2nd ed. New York: John Wiley & Sons.

Corbett, S.S. & Drewett, R.F. (2004) To what extent is failure to thrive in infancy associated with poorer cognitive development? A review and meta-analysis. *J Child Psychol Psychiatry*, **45**, 641-654.

Corcoran, K.A. & Quirk, G.J. (2007) Recalling safety: cooperative functions of the ventromedial prefrontal cortex and the hippocampus in extinction. *CNS Spectr*, **12**, 200-206.

Courtin, J., Chaudun, F., Rozeske, R.R., Karalis, N., Gonzalez-Campo, C., Wurtz, H., Abdi, A., Baufreton, J., Bienvenu, T.C. & Herry, C. (2014) Prefrontal parvalbumin interneurons shape neuronal activity to drive fear expression. *Nature*, **505**, 92-96.

Cressman, V.L., Balaban, J., Steinfeld, S., Shemyakin, A., Graham, P., Parisot, N. & Moore, H. (2010) Prefrontal cortical inputs to the basal amygdala undergo pruning during late adolescence in the rat. *J Comp Neurol*, **518**, 2693-2709.

Cummings, K.A. & Clem, R.L. (2020) Prefrontal somatostatin interneurons encode fear memory. *Nat Neurosci*, **23**, 61-74.

Cunningham, M.G., Bhattacharyya, S. & Benes, F.M. (2002) Amygdalo-cortical sprouting continues into early adulthood: implications for the development of normal and abnormal function during adolescence. *J Comp Neurol*, **453**, 116-130.

del Río, J.A., de Lecea, L., Ferrer, I. & Soriano, E. (1994) The development of parvalbumin-immunoreactivity in the neocortex of the mouse. *Brain Res Dev Brain Res*, **81**, 247-259.

Do-Monte, F.H., Manzano-Nieves, G., Quinones-Laracuente, K., Ramos-Medina, L. & Quirk, G.J. (2015) Revisiting the role of infralimbic cortex in fear extinction with optogenetics. *J Neurosci*, **35**, 3607-3615.

Drzewiecki, C.M. & Juraska, J.M. (2020) The structural reorganization of the prefrontal cortex during adolescence as a framework for vulnerability to the environment. *Pharmacol Biochem Behav*, **199**, 173044.

Ehrlich, D.E., Ryan, S.J. & Rainnie, D.G. (2012) Postnatal development of electrophysiological properties of principal neurons in the rat basolateral amygdala. *J Physiol*, **590**, 4819-4838.

Farrell, M.R., Holland, F.H., Shansky, R.M. & Brenhouse, H.C. (2016) Sex-specific effects of early life stress on social interaction and prefrontal cortex dendritic morphology in young rats. *Behav Brain Res*, **310**, 119-125.

Fitzgerald, P.J., Giustino, T.F., Seemann, J.R. & Maren, S. (2015) Noradrenergic blockade stabilizes prefrontal activity and enables fear extinction under stress. *Proc Natl Acad Sci U S A*, **112**, E3729-3737.

Ganguly, P., Thompson, V., Gildawie, K. & Brenhouse, H.C. (2018) Adolescent food restriction in rats alters prefrontal cortex microglia in an experience-dependent manner. *Stress*, **21**,

162-168.

Gee, D.G., Gabard-Durnam, L.J., Flannery, J., Goff, B., Humphreys, K.L., Telzer, E.H., Hare, T.A., Bookheimer, S.Y. & Tottenham, N. (2013) Early developmental emergence of human amygdala-prefrontal connectivity after maternal deprivation. *Proc Natl Acad Sci U S A*, **110**, 15638-15643.

Gildawie, K.R., Honeycutt, J.A. & Brenhouse, H.C. (2020) Region-specific Effects of Maternal Separation on Perineuronal Net and Parvalbumin-expressing Interneuron Formation in Male and Female Rats. *Neuroscience*, **428**, 23-37.

Gildawie, K.R., Ryll, L.M., Hexter, J.C., Peterzell, S., Valentine, A.A. & Brenhouse, H.C. (2021) A two-hit adversity model in developing rats reveals sex-specific impacts on prefrontal cortex structure and behavior. *Dev Cogn Neurosci*, **48**, 100924.

Giustino, T.F. & Maren, S. (2015) The Role of the Medial Prefrontal Cortex in the Conditioning and Extinction of Fear. *Front Behav Neurosci*, **9**, 298.

González-Pardo, H., Arias, J.L., Gómez-Lázaro, E., López Taboada, I. & Conejo, N.M. (2020) Sex-Specific Effects of Early Life Stress on Brain Mitochondrial Function, Monoamine Levels and Neuroinflammation. *Brain Sci*, **10**.

Grassi-Oliveira, R., Honeycutt, J.A., Holland, F.H., Ganguly, P. & Brenhouse, H.C. (2016) Cognitive impairment effects of early life stress in adolescents can be predicted with early biomarkers: Impacts of sex, experience, and cytokines. *Psychoneuroendocrinology*, **71**, 19-30.

Guadagno, A., Belliveau, C., Mechawar, N. & Walker, C.D. (2021) Effects of Early Life Stress on the Developing Basolateral Amygdala-Prefrontal Cortex Circuit: The Emerging Role of Local Inhibition and Perineuronal Nets. *Front Hum Neurosci*, **15**, 669120.

Guadagno, A., Kang, M.S., Devenyi, G.A., Mathieu, A.P., Rosa-Neto, P., Chakravarty, M. & Walker, C.D. (2018a) Reduced resting-state functional connectivity of the basolateral amygdala to the medial prefrontal cortex in preweaning rats exposed to chronic early-life stress. *Brain Struct Funct*, **223**, 3711-3729.

Guadagno, A., Verlezza, S., Long, H., Wong, T.P. & Walker, C.D. (2020) It Is All in the Right Amygdala: Increased Synaptic Plasticity and Perineuronal Nets in Male, But Not Female, Juvenile Rat Pups after Exposure to Early-Life Stress. *J Neurosci*, **40**, 8276-8291.

Guadagno, A., Wong, T.P. & Walker, C.D. (2018b) Morphological and functional changes in the preweaning basolateral amygdala induced by early chronic stress associate with anxiety and fear behavior in adult male, but not female rats. *Prog Neuropsychopharmacol Biol Psychiatry*, **81**, 25-37.

Hensch, T.K. (2005) Critical period mechanisms in developing visual cortex. *Curr Top Dev Biol*, **69**, 215-237.

Herry, C., Ciocchi, S., Senn, V., Demmou, L., Müller, C. & Lüthi, A. (2008) Switching on and off fear by distinct neuronal circuits. *Nature*, **454**, 600-606.

Herzberg, M.P. & Gunnar, M.R. (2020) Early life stress and brain function: Activity and connectivity associated with processing emotion and reward. *Neuroimage*, **209**, 116493.

Honeycutt, J.A., Demaestri, C., Peterzell, S., Silveri, M.M., Cai, X., Kulkarni, P., Cunningham, M.G., Ferris, C.F. & Brenhouse, H.C. (2020) Altered corticolimbic connectivity reveals sex-specific adolescent outcomes in a rat model of early life adversity. *Elife*, **9**.

Hoover, W.B. & Vertes, R.P. (2007) Anatomical analysis of afferent projections to the medial prefrontal cortex in the rat. *Brain Struct Funct*, **212**, 149-179.

Hu, H., Gan, J. & Jonas, P. (2014) Interneurons. Fast-spiking, parvalbumin^{+} GABAergic interneurons: from cellular design to microcircuit function. *Science*, **345**, 1255263.

Hu, J.S., Vogt, D., Sandberg, M. & Rubenstein, J.L. (2017) Cortical interneuron development: a tale of time and space. *Development*, **144**, 3867-3878.

Hübner, C., Bosch, D., Gall, A., Lüthi, A. & Ehrlich, I. (2014) Ex vivo dissection of optogenetically activated mPFC and hippocampal inputs to neurons in the basolateral amygdala: implications for fear and emotional memory. *Front Behav Neurosci*, **8**, 64.

Hugues, S. & Garcia, R. (2007) Reorganization of learning-associated prefrontal synaptic plasticity between the recall of recent and remote fear extinction memory. *Learn Mem*, **14**, 520-524.

Hylin, M.J., Orsi, S.A., Moore, A.N. & Dash, P.K. (2013) Disruption of the perineuronal net in the hippocampus or medial prefrontal cortex impairs fear conditioning. *Learn Mem*, **20**, 267-273.

Ji, G. & Neugebauer, V. (2012) Modulation of medial prefrontal cortical activity using in vivo

recordings and optogenetics. *Mol Brain*, **5**, 36.

Johnson, F.K., Delpech, J.C., Thompson, G.J., Wei, L., Hao, J., Herman, P., Hyder, F. & Kaffman, A. (2018) Amygdala hyper-connectivity in a mouse model of unpredictable early life stress. *Transl Psychiatry*, **8**, 49.

Johnson, F.K. & Kaffman, A. (2018) Early life stress perturbs the function of microglia in the developing rodent brain: New insights and future challenges. *Brain Behav Immun*, **69**, 18-27.

Jovanovic, T., Nylocks, K.M. & Gamwell, K.L. (2013) Translational neuroscience measures of fear conditioning across development: applications to high-risk children and adolescents. *Biol Mood Anxiety Disord*, **3**, 17.

Junod, A., Opendak, M., LeDoux, J.E. & Sullivan, R.M. (2019) Development of Threat Expression Following Infant Maltreatment: Infant and Adult Enhancement but Adolescent Attenuation. *Front Behav Neurosci*, **13**, 130.

Lee, Y.K. & Choi, J.S. (2012) Inactivation of the medial prefrontal cortex interferes with the expression but not the acquisition of differential fear conditioning in rats. *Exp Neurobiol*, **21**, 23-29.

Little, J.P. & Carter, A.G. (2013) Synaptic mechanisms underlying strong reciprocal connectivity between the medial prefrontal cortex and basolateral amygdala. *J Neurosci*, **33**, 15333-15342.

Liu, X. & Carter, A.G. (2018) Ventral Hippocampal Inputs Preferentially Drive Corticocortical Neurons in the Infralimbic Prefrontal Cortex. *J Neurosci*, **38**, 7351-7363.

Lucas, E.K. & Clem, R.L. (2018) GABAergic interneurons: The orchestra or the conductor in fear learning and memory? *Brain Res Bull*, **141**, 13-19.

Luczynski, P., Moquin, L. & Gratton, A. (2015) Chronic stress alters the dendritic morphology of callosal neurons and the acute glutamate stress response in the rat medial prefrontal cortex. *Stress*, **18**, 654-667.

Majcher-Maślanka, I., Solarz, A., Wędzony, K. & Chocyk, A. (2018) Previous Early-life Stress Modifies Acute Corticosterone-induced Synaptic Plasticity in the Medial Prefrontal Cortex of Adolescent Rats. *Neuroscience*, **379**, 316-333.

Manzano Nieves, G., Bravo, M., Baskoylu, S. & Bath, K.G. (2020) Early life adversity decreases pre-adolescent fear expression by accelerating amygdala PV cell development. *Elife*, **9**.

Marek, R., Jin, J., Goode, T.D., Giustino, T.F., Wang, Q., Acca, G.M., Holehonnur, R., Ploski, J.E., Fitzgerald, P.J., Lynagh, T., Lynch, J.W., Maren, S. & Sah, P. (2018a) Hippocampus-driven feed-forward inhibition of the prefrontal cortex mediates relapse of extinguished fear. *Nat Neurosci*, **21**, 384-392.

Marek, R., Sun, Y. & Sah, P. (2019) Neural circuits for a top-down control of fear and extinction. *Psychopharmacology (Berl)*, **236**, 313-320.

Marek, R., Xu, L., Sullivan, R.K.P. & Sah, P. (2018b) Excitatory connections between the prelimbic and infralimbic medial prefrontal cortex show a role for the prelimbic cortex in fear extinction. *Nat Neurosci*, **21**, 654-658.

Markham, J.A., Morris, J.R. & Juraska, J.M. (2007) Neuron number decreases in the rat ventral, but not dorsal, medial prefrontal cortex between adolescence and adulthood. *Neuroscience*, **144**, 961-968.

Marowsky, A., Yanagawa, Y., Obata, K. & Vogt, K.E. (2005) A specialized subclass of interneurons mediates dopaminergic facilitation of amygdala function. *Neuron*, **48**, 1025-1037.

McLaughlin, R.J., Verlezza, S., Gray, J.M., Hill, M.N. & Walker, C.D. (2016) Inhibition of anandamide hydrolysis dampens the neuroendocrine response to stress in neonatal rats subjected to suboptimal rearing conditions. *Stress*, **19**, 114-124.

Milad, M.R. & Quirk, G.J. (2002) Neurons in medial prefrontal cortex signal memory for fear extinction. *Nature*, **420**, 70-74.

Molet, J., Maras, P.M., Avishai-Eliner, S. & Baram, T.Z. (2014) Naturalistic rodent models of chronic early-life stress. *Dev Psychobiol*, **56**, 1675-1688.

Monroy, E., Hernández-Torres, E. & Flores, G. (2010) Maternal separation disrupts dendritic morphology of neurons in prefrontal cortex, hippocampus, and nucleus accumbens in male rat offspring. *J Chem Neuroanat*, **40**, 93-101.

Moryś, J., Berdel, B., Kowiański, P. & Dziewiatkowski, J. (1998) The pattern of synaptophysin changes during the maturation of the amygdaloid body and hippocampal hilus in the rat. *Folia Neuropathol*, **36**, 15-23.

Moussaoui, N., Jacobs, J.P., Larauche, M., Biraud, M., Million, M., Mayer, E. & Taché, Y. (2017) Chronic Early-life Stress in Rat Pups Alters Basal Corticosterone, Intestinal Permeability, and Fecal Microbiota at Weaning: Influence of Sex. *J Neurogastroenterol Motil*, **23**, 135-143.

Muhammad, A. & Kolb, B. (2011) Maternal separation altered behavior and neuronal spine density without influencing amphetamine sensitization. *Behav Brain Res*, **223**, 7-16.

Myers, K.M. & Davis, M. (2007) Mechanisms of fear extinction. *Mol Psychiatry*, **12**, 120-150.

O'Connor, R.M., Moloney, R.D., Glennon, J., Vlachou, S. & Cryan, J.F. (2015) Enhancing glutamatergic transmission during adolescence reverses early-life stress-induced deficits in the rewarding effects of cocaine in rats. *Neuropharmacology*, **99**, 168-176.

Orsini, C.A. & Maren, S. (2012) Neural and cellular mechanisms of fear and extinction memory formation. *Neurosci Biobehav Rev*, **36**, 1773-1802.

Ovtscharoff, W., Jr. & Braun, K. (2001) Maternal separation and social isolation modulate the postnatal development of synaptic composition in the infralimbic cortex of Octodon degus. *Neuroscience*, **104**, 33-40.

Paré, D., Quirk, G.J. & Ledoux, J.E. (2004) New vistas on amygdala networks in conditioned fear. *J Neurophysiol*, **92**, 1-9.

Pattwell, S.S., Bath, K.G., Casey, B.J., Ninan, I. & Lee, F.S. (2011) Selective early-acquired fear memories undergo temporary suppression during adolescence. *Proc Natl Acad Sci U S A*, **108**, 1182-1187.

Pattwell, S.S., Duhoux, S., Hartley, C.A., Johnson, D.C., Jing, D., Elliott, M.D., Ruberry, E.J., Powers, A., Mehta, N., Yang, R.R., Soliman, F., Glatt, C.E., Casey, B.J., Ninan, I. & Lee, F.S. (2012) Altered fear learning across development in both mouse and human. *Proc Natl Acad Sci U S A*, **109**, 16318-16323.

Pattwell, S.S., Liston, C., Jing, D., Ninan, I., Yang, R.R., Witztum, J., Murdock, M.H., Dincheva, I., Bath, K.G., Casey, B.J., Deisseroth, K. & Lee, F.S. (2016) Dynamic changes in neural circuitry during adolescence are associated with persistent attenuation of fear memories. *Nat Commun*, **7**, 11475.

Paxinos, G., Watson, C., 2005. The Rat Brain in Stereotaxic Coordinates. Elservier, Amsterdam;

Boston

Pechtel, P. & Pizzagalli, D.A. (2011) Effects of early life stress on cognitive and affective function: an integrated review of human literature. *Psychopharmacology (Berl)*, **214**, 55-70.

Prusator, D.K. & Greenwood-Van Meerveld, B. (2016) Sex-related differences in pain behaviors following three early life stress paradigms. *Biol Sex Differ*, **7**, 29.

Rau, A.R., Chappell, A.M., Butler, T.R., Ariwodola, O.J. & Weiner, J.L. (2015) Increased Basolateral Amygdala Pyramidal Cell Excitability May Contribute to the Anxiogenic Phenotype Induced by Chronic Early-Life Stress. *J Neurosci*, **35**, 9730-9740.

Reh, R.K., Dias, B.G., Nelson, C.A., 3rd, Kaufer, D., Werker, J.F., Kolb, B., Levine, J.D. & Hensch, T.K. (2020) Critical period regulation across multiple timescales. *Proc Natl Acad Sci U S A*, **117**, 23242-23251.

Reincke, S.A. & Hanganu-Opatz, I.L. (2017) Early-life stress impairs recognition memory and perturbs the functional maturation of prefrontal-hippocampal-perirhinal networks. *Sci Rep*, **7**, 42042.

Ruden, J.B., Dugan, L.L. & Konradi, C. (2021) Parvalbumin interneuron vulnerability and brain disorders. *Neuropsychopharmacology*, **46**, 279-287.

Rudy, B., Fishell, G., Lee, S. & Hjerling-Leffler, J. (2011) Three groups of interneurons account for nearly 100% of neocortical GABAergic neurons. *Dev Neurobiol*, **71**, 45-61.

Ryan, S.J., Ehrlich, D.E. & Rainnie, D.G. (2016) Morphology and dendritic maturation of developing principal neurons in the rat basolateral amygdala. *Brain Struct Funct*, **221**, 839-854.

Senn, V., Wolff, S.B., Herry, C., Grenier, F., Ehrlich, I., Gründemann, J., Fadok, J.P., Müller, C., Letzkus, J.J. & Lüthi, A. (2014) Long-range connectivity defines behavioral specificity of amygdala neurons. *Neuron*, **81**, 428-437.

Sierra-Mercado, D., Padilla-Coreano, N. & Quirk, G.J. (2011) Dissociable roles of prelimbic and infralimbic cortices, ventral hippocampus, and basolateral amygdala in the expression and extinction of conditioned fear. *Neuropsychopharmacology*, **36**, 529-538.

Sohal, V.S., Zhang, F., Yizhar, O. & Deisseroth, K. (2009) Parvalbumin neurons and gamma

rhythms enhance cortical circuit performance. *Nature*, **459**, 698-702.

Sotres-Bayon, F., Sierra-Mercado, D., Pardilla-Delgado, E. & Quirk, G.J. (2012) Gating of fear in prelimbic cortex by hippocampal and amygdala inputs. *Neuron*, **76**, 804-812.

Spampanato, J., Polepalli, J. & Sah, P. (2011) Interneurons in the basolateral amygdala. *Neuropharmacology*, **60**, 765-773.

Stevenson, C.W., Spicer, C.H., Mason, R. & Marsden, C.A. (2009) Early life programming of fear conditioning and extinction in adult male rats. *Behav Brain Res*, **205**, 505-510.

Strobel, C., Marek, R., Gooch, H.M., Sullivan, R.K.P. & Sah, P. (2015) Prefrontal and Auditory Input to Intercalated Neurons of the Amygdala. *Cell Rep*, **10**, 1435-1442.

Thomases, D.R., Cass, D.K., Meyer, J.D., Caballero, A. & Tseng, K.Y. (2014) Early adolescent MK-801 exposure impairs the maturation of ventral hippocampal control of basolateral amygdala drive in the adult prefrontal cortex. *J Neurosci*, **34**, 9059-9066.

Thomases, D.R., Cass, D.K. & Tseng, K.Y. (2013) Periadolescent exposure to the NMDA receptor antagonist MK-801 impairs the functional maturation of local GABAergic circuits in the adult prefrontal cortex. *J Neurosci*, **33**, 26-34.

Tottenham, N. (2020) Early Adversity and the Neotenous Human Brain. *Biol Psychiatry*, **87**, 350-358.

Tovote, P., Fadok, J.P. & Luthi, A. (2015) Neuronal circuits for fear and anxiety. *Nat Rev Neurosci*, **16**, 317-331.

Tremblay, R., Lee, S. & Rudy, B. (2016) GABAergic Interneurons in the Neocortex: From Cellular Properties to Circuits. *Neuron*, **91**, 260-292.

Van Eden, C.G. & Uylings, H.B. (1985) Postnatal volumetric development of the prefrontal cortex in the rat. *J Comp Neurol*, **241**, 268-274.

VanTieghem, M.R. & Tottenham, N. (2018) Neurobiological Programming of Early Life Stress: Functional Development of Amygdala-Prefrontal Circuitry and Vulnerability for Stress-Related Psychopathology. *Curr Top Behav Neurosci*, **38**, 117-136.

Verwer, R.W., Van Vulpen, E.H. & Van Uum, J.F. (1996) Postnatal development of amygdaloid projections to the prefrontal cortex in the rat studied with retrograde and anterograde

tracers. *J Comp Neurol*, **376**, 75-96.

Vidal-Gonzalez, I., Vidal-Gonzalez, B., Rauch, S.L. & Quirk, G.J. (2006) Microstimulation reveals opposing influences of prelimbic and infralimbic cortex on the expression of conditioned fear. *Learn Mem*, **13**, 728-733.

Walker, C.D., Bath, K.G., Joels, M., Korosi, A., Larauche, M., Lucassen, P.J., Morris, M.J., Raineki, C., Roth, T.L., Sullivan, R.M., Tache, Y. & Baram, T.Z. (2017) Chronic early life stress induced by limited bedding and nesting (LBN) material in rodents: critical considerations of methodology, outcomes and translational potential. *Stress*, **20**, 421-448.

White, J.D., Arefin, T.M., Pugliese, A., Lee, C.H., Gassen, J., Zhang, J. & Kaffman, A. (2020) Early life stress causes sex-specific changes in adult fronto-limbic connectivity that differentially drive learning. *Elife*, **9**.

Wonders, C.P. & Anderson, S.A. (2006) The origin and specification of cortical interneurons. *Nat Rev Neurosci*, **7**, 687-696.

Yang, S.S., Mack, N.R., Shu, Y. & Gao, W.J. (2021) Prefrontal GABAergic Interneurons Gate Long-Range Afferents to Regulate Prefrontal Cortex-Associated Complex Behaviors. *Front Neural Circuits*, **15**, 716408.

Yizhar, O. & Klavir, O. (2018) Reciprocal amygdala-prefrontal interactions in learning. *Curr Opin Neurobiol*, **52**, 149-155.

Zimmermann, K.S., Richardson, R. & Baker, K.D. (2019) Maturational Changes in Prefrontal and Amygdala Circuits in Adolescence: Implications for Understanding Fear Inhibition during a Vulnerable Period of Development. *Brain Sci*, **9**.

I. Ethnical Approval

McGill

November 10, 2021

Animal Certificate

This is to certify that **Dr. Claire Dominique Walker, Department of Psychiatry, Douglas Mental Health University Institute,** currently holds an approved **Animal Use Protocol # 2020-8179** with McGill University and its Affiliated Hospital's Research Institutes for the following project:

Animal Use Protocol Title: Sex-dependent effects of early life stress on the development of the basolateral amygdala-prefrontal cortex circuit for fear conditioning

Start date: October 1, 2021

Expiration date: September 30, 2022

McGill University and Affiliated Hospitals Research Institutes recognize the importance of animal research in our efforts to further our knowledge of natural processes, diseases and conservation. Research, educational and testing projects are conducted with full commitment to the wellbeing of the animal subjects. In order to limit animal use to meritorious research or educational projects, the institution relies on stringent peer review processes, along with assessment of ethical issues by the Animal Care Committee. McGill University recognizes that the use of animals in research, teaching and testing carries significant responsibilities. The institution will continue to develop and maintain guidelines and regulations, following the high standards established by the Canadian Council on Animal Care. It is committed to conducting the highest-quality research and to providing animals with the best care.

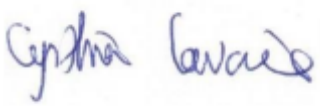

Cynthia Lavoie
Animal Ethics and Compliance Administrator
Animal Compliance Office
Office of Vice-Principal (Research and Innovation)
Suite 325, James Administration Building, McGill University
845 Sherbrooke Street West, Montreal, Quebec, Canada H3A 0G4
animal.approvals@mcgill.ca

McGill

October 1, 2020

Animal Certificate

This is to certify that **Dr. Claire Dominique Walker, Department of Psychiatry, Douglas Mental Health University Institute,** currently holds an approved **Animal Use Protocol # 2020-8179** with McGill University and its Affiliated Hospital's Research Institutes for the following project:

Animal Use Protocol Title: Sex-dependent effects of early life stress on the development of the basolateral amygdala-prefrontal cortex circuit for fear conditioning

Start date: October 1, 2020

Expiration date: September 30, 2021

McGill University and Affiliated Hospitals Research Institutes recognize the importance of animal research in our efforts to further our knowledge of natural processes, diseases and conservation. Research, educational and testing projects are conducted with full commitment to the wellbeing of the animal subjects. In order to limit animal use to meritorious research or educational projects, the institution relies on stringent peer review processes, along with assessment of ethical issues by the Animal Care Committee. McGill University recognizes that the use of animals in research, teaching and testing carries significant responsibilities. The institution will continue to develop and maintain guidelines and regulations, following the high standards established by the Canadian Council on Animal Care. It is committed to conducting the highest-quality research and to providing animals with the best care.

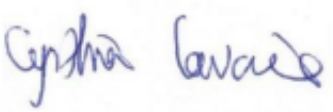

Cynthia Lavoie
Animal Ethics and Compliance Administrator
Animal Compliance Office
Office of Vice-Principal (Research and Innovation)
Suite 325, James Administration Building, McGill University
845 Sherbrooke Street West, Montreal, Quebec, Canada H3A 0G4
animal.approvals@mcgill.ca